Investigating the mechanics of N4BP1 in mammalian cells

by

Zane Brown

A thesis submitted in partial fulfillment of the requirements for the degree of M.Sc.

at

McGill University

Montreal, Quebec

July 2021

Table of contents

List of figures and tables

List of abbreviations

Ago2 ..... Argonaut 2

BSA..... Bovine serum albumin

CCR4-NOT ..... Carbon catabolite repression 4-negative on TATA-less

cDNA ..... Complementary DNA

CoCUN ..... Cousin of cullin-binding domain associated with NEDD8

CRAPome ..... Contaminant repository for affinity purification

DCP ..... Decapping mRNA

DDX6 ..... Deadbox helicase 6

DNA ..... Deoxyribonucleic acid

DNase ..... Deoxyribonuclease

dNTP ..... Deoxyribonucleotide triphosphate

dsRBM ..... Double-stranded RNA binding motif

EDC ..... Enhancer of decapping

eIF2α ..... Eukaryotic initiation factor 2α

FL ..... Firefly luciferase

HeLa ..... Henrietta Lacks

HEK-293T ..... Human embryonic kidney 293T

HFV ..... Human foamy virus

HIV ..... Human immunodeficiency virus

IFN ..... Interferon

KH ..... K-homology

MARF1 ..... Meiosis regulator and mRNA stability factor 1

MALT1 ..... Mucosa-associated lymphoid tissue lymphoma translocation protein 1

MEF ..... Mouse embryonic fibroblast

MHC ..... Major histocompatibility complex

miRISC ..... miRNA-induced silencing complex

miRNA ..... Micro-RNA

MLV .....Murine leukemia virus

mRNA ..... Messenger RNA

NEMO .....NF-κB essential modulator

NF-κB ..... Nuclear factor κB

NYN ..... N4BP1 YacP-like nuclease

N4BP1 .....Nedd4 binding protein 1

PABP .....Poly(A) binding protein

Pan ..... Poly(A) specific ribonuclease

PBS .....Phosphate buffered saline

PEI .....Polyethylenimine

PIC .....Protease inhibitor cocktail

PIN .....PilT N-terminal RNase-like

PML ..... Promyelocytic

PRORP1 .....Proteinaceous RNase P1

P-body .....Processing body

qPCR ..... Quantitative polymerase chain reaction

RL .....Renilla luciferase

RNase ..... Ribonuclease

RNA .....Ribonucleic acid

RRM .....RNA recognition motif

rRNA ..... Ribosomal RNA

RT .....Room temperature

RT-qPCR .....Real time qPCR

SDS-PAGE .....Sodium dodecyl sulfate-polyacrylamide gel electrophoresis

SF1 ..... Splicing factor 1

SG ..... Stress granule

SIV ..... Simian immunodeficiency virus

SUMO ..... Small ubiquitin like modifier

TLR ..... Toll-like receptor

TBS .....Tris buffered saline

TNF .....Tumour necrosis factor

TRAF ..... Tumour necrosis factor receptor associated factor

TUT ..... Terminal uridyltransferase

U-2 OS ..... Human bone osteosarcoma epithelial

WT .....Wild-type

Xrn1 ..... 5'-3' exonuclease

ZAP ..... Zinc finger antiviral protein

ZF .....Zinc finger

ΔNYN .....NYN domain deleted

Acknowledgements

My time working on this project has pushed me to grow so much, and helped me to accomplish things I wasn't sure I could. I couldn't be more grateful for all the people who have helped me along the way.

Firstly, to my supervisor Dr. Marc Fabian. I recall when I first came into the lab to be interviewed, I was taken in by your energy. You were so involved in the lab, knowing everyone's project and progress, and checking in on how people were doing. Having you present in the lab was something that I valued so greatly, as we worked through the many ups and downs of my project. Most of all, when I was having a tough time you were supportive and allowed me to do what was needed to move forward positively – I will always be thankful for that.

To my colleagues Benedeta, Sahil, Sam and Will – you were among the most important reasons I chose to come to this lab; you were what helped me truly enjoy this experience. You taught me the science from the ground up, and always brought a smile to my face. Benedeta – you were the best lab mom, thank you for always looking out for us. Sahil – you're an amazing person, and I really appreciate the support you've given to me. Sam – I'm so grateful for how close we have gotten, and I feel as though I've matured so much by working with you. Will – you've been an amazing mentor/friend, thanks for showing me the ropes.

I would like to thank my committee members Dr. Selena Sagan and Dr. Rongtuan Lin for their guidance and support throughout my project. Your feedback has been critical to the progression of my work.

I have gotten so close to so many people in the Lady Davis Institute, and the friendliness of everyone there was something I will never forget. While I can't name everyone specifically, I'm very thankful for having all of you amazing people in my life.

Finally and most of all, to Ma, Pa and Shael – I'm not sure if you knew what you signed up for when you said you would always be there for me, but I truly would not be at this point without you. Thank you. It is amazing that after everything that's happened, we can look at this happy future together. To my friends (Brad, Yael, Nicole, Ben, Max, Pete) and family (Sam, Joey and Bess), each of you has contributed to helping me being the person I am today, and your love has helped so much in me finishing this degree.

Contribution of authors

Dr. Marc Fabian conceived of the outlined project, and revised the written portion of this thesis. Mass spectrometry analysis was conducted by the Lady Davis Institute proteomics core (Montreal, QC). Zane Brown carried out all remaining experiments, data analysis, and writing found in this document. William Brothers acted as a key mentor in the undertaking of experiments.

Abstract

The bulk of mRNA turnover proceeds through a deadenylation dependent mechanism, whereby mRNAs have their 3'-poly(A) tails trimmed, followed by either degradation by the 3'-5' exosome, or decapping of the 5' end and degradation by the 5'-3' exonuclease Xrn1 (5'-3' exonuclease 1). However, several mechanisms exist to specifically regulate subsets of mRNAs, allowing for fine-tuning of the transcriptome by deadenylation-independent mRNA decay. One such mechanism is via endonucleases that internally cleave RNA to promote decay and play key roles in controlling specific transcripts. Recently, a novel class of predicted nuclease domains were identified, known as NYN domains. One such protein encoding this domain is N4BP1, which is upregulated in immune cells upon interferon stimulation. This protein contains a predicted RNA binding KH (K-homology) domain as well as a C-terminal NYN and ubiquitin binding domains. N4BP1 has been shown to directly repress HIV RNAs dependent on its NYN domain. However, whether N4BP1 can target and repress polyadenylated mRNAs remains unclear.

This project set out to investigate the role of N4BP1 in mammalian cells, specifically silencing activity, cellular localization and identifying N4BP1-associated proteins. A number of N4BP1 mutants were artificially tethered to reporter mRNAs in order to assess whether N4BP1 can repress protein synthesis of target mRNAs using dual-luciferase reporter assays. We observed that N4BP1 repression is dependent on its NYN domain, and N4BP1 induces repression similar to that observed for other *bona fide* NYN domain endonucleases. Immunofluorescence and cell fractionation analyses were carried out to investigate how ectopic N4BP1 localizes in human cell lines. This study shows that N4BP1 can localize both to the cytosol and to the nucleus in HeLa and U-2 OS cell lines. What is more, N4BP1 can form foci,

co-localizing with components of processing (P)-bodies in the cytosol. While the N-terminal region of N4BP1 alone was able to co-localize with processing P-body proteins, the central (linker) region of this protein was the only fragment of N4BP1 that appeared in the nucleus. Preliminary
proteomic analyses were also carried out to identify N4BP1-associating proteins in U-2 OS and HeLa cell lines. Taken together, the data in this thesis support the notion that N4BP1 post-transcriptionally regulates gene expression by destabilizing mRNAs, and that it localizes to P-bodies via its N-terminal KH domain.

Résumé

La majeure partie du renouvellement de l'ARNm passe par un mécanisme dépendant de la déadénylation, par lequel les ARNm ont leurs queues 3'-poly (A) coupées, suivies soit d'une dégradation par l'exosome 3'-5', soit d'un décapage de l'extrémité 5' et d'une dégradation par le 5'-3' exonucléase Xrn1. Cependant, plusieurs mécanismes existent pour réguler spécifiquement les sous-ensembles d'ARNm, permettant un réglage fin du transcriptome par la dés-adénylation indépendante de la désintégration de l'ARNm. L'un de ces mécanismes se fait via des endonucléases qui clivent de manière interne l'ARN pour favoriser la désintégration et jouent un rôle clé dans le contrôle de transcrits spécifiques. Récemment, une nouvelle classe de domaines de nucléase prédits a été identifiée, connue sous le nom de domaines NYN. L'une de ces protéines codant pour ce domaine est N4BP1, qui est induite dans les cellules immunitaires lors de la stimulation par l'interféron. Cette protéine contient un domaine KH de liaison à l'ARN ainsi que des domaines de liaison C-terminaux NYN et ubiquitine. Il a été démontré que N4BP1 réprime directement les ARN du VIH par l'intermédiaire de son domaine NYN. Cependant, on ne sait pas si N4BP1 peut cibler et réprimer les ARNm polyadénylés.

Ce projet visait à étudier le rôle de N4BP1 dans les cellules de mammifères, en particulier l'activité d'extinction de gènes, la localisation cellulaire et l'identification des protéines associées à N4BP1. Un certain nombre de mutants N4BP1 ont été artificiellement attachés à des ARNm rapporteurs afin d'évaluer si N4BP1 peut réprimer la synthèse protéique des ARNm cibles en utilisant des tests de rapporteur à double luciférase. Nous avons observé que la répression de N4BP1 dépend de son domaine NYN, et que N4BP1 induit une répression similaire à celle observée pour d'autres endonucléases authentiques du domaine NYN. Des analyses

d'immunofluorescence et de fractionnement cellulaire ont été effectuées pour étudier comment le N4BP1 ectopique se localise dans les lignées cellulaires humaines. Cette étude montre que N4BP1 peut être localisée localiser à la fois le cytosol et le noyau dans les lignées cellulaires HeLa et U-2 OS. De plus, N4BP1 peut former des foyers, co-localisés avec des composants des corps de transformation (P) dans le cytosol. Alors que la région N-terminale de N4BP1 seule était capable de co-localiser avec les protéines du corps P de traitement, la région centrale (de liaison) de cette protéine était le seul fragment de N4BP1 qui apparaissait dans le noyau. Des analyses protéomiques préliminaires ont également été effectuées pour identifier les protéines associées à N4BP1 dans les lignées cellulaires U-2 OS et HeLa. Prises ensemble, les données de cette thèse soutiennent l'hypothèse que N4BP1 régule de manière post-transcriptionnelle l'expression des gènes en déstabilisant les ARNm, et qu'elle se localise sur les corps P via son domaine KH N-terminal.

Introduction

1.1 Eukaryotic mRNA regulation

The regulated decay of eukaryotic mRNAs plays an important role in the post-transcriptional control of gene expression (Beelman & Parker, 1995). It is essential that cells can rapidly and specifically regulate the levels of specific transcripts to respond effectively to changing internal and external conditions. This regulation is accomplished through various mechanisms, including translational repression [e.g. by eukaryotic initiation factor 2α, (eIF2α) during the stress response], deadenylation-dependent mRNA decay and various ribonucleases (Decker & Parker, 1993, Scheuner et al., 2001, Novoa et al., 2001, Uehata et al., 2013). There is significant overlap between these processes, often with various components being used for multiple decay pathways. Further, repressing gene expression can occur through two events - decay of mRNA or blocking the ability of intact transcripts to be translated (Decker & Parker, 1993, Scheuner et al., 2001, Novoa et al., 2001).

The majority of mRNA turnover pathways begins with the deadenylation of the 3' poly(A) tail of the transcript (Muhlrad et al., 1994, Łabno et al., 2016) (Figure 1). The major deadenylase complexes are CCR4-NOT (Carbon catabolite repression 4-negative on TATA-less) and Pan2/Pan3 (poly(A) specific ribonuclease) which collaborate to trim short and long poly(A) tails, respectively (Yi et al., 2018). Subsequently, the protective 5'-methylguanosine cap is hydrolyzed by the DCP2 (decapping mRNA 2). Decapped mRNAs can then be fully broken down either by XRN1 (5'-3' exonuclease) or the exosome complex (3'-5' exonuclease) (Muhlrad et al., 1994). Beyond the enzymes listed above, there are many other proteins which are required for mRNA decay. For example, poly(A)-binding protein (PABPC1) protects the mRNA from being degraded, but also interacts with PAN3, one of the deadenylating enzymes (Schäfer et al., 2019).

To functionally link deadenylation to decapping, shortened poly(A) tails can be uridylated by terminal uridyltransferases (TUT4/7), which interact with the LSM1-7 complex (Tharun, 2009). Importantly, PATL1 binds the LSM1-7 complex as well as components of decapping machinery including DDX6 (DEADbox helicase 6) and DCP1/2, facilitating the initiation of mRNA decapping (Ozgur et al., 2010, Braun et al., 2010). Further, many proteins are required for efficient mRNA decapping by DCP2, including DCP1 and enhancer of decapping (EDC) proteins such as EDC4 (Chang et al., 2014). The complexity of the deadenylation-dependent RNA decay pathway illustrates a common theme in RNA decay – tight regulation is key to efficiently and specifically manage the transcriptome.

Importantly, several other pathways exist that post-transcriptionally regulate gene expression. When transcripts prematurely terminate translation, they are degraded by nonsense-mediated decay or no-go decay pathways (Losson & Lacroute, 1979, Harigaya & Parker, 2010). Further, mRNAs can be targeted in a sequence-specific manner through micro (mi)RNA-mediated silencing, where complementary miRNAs (micro-RNAs) guide the miRNA-induced silencing complex (miRISC), to target mRNAs and block protein synthesis (Bouasker & Simard, 2012, Liu et al., 2004). Altogether, the many pathways of mRNA decay and repression work together to regulate the transcriptome both in bulk and with specific targets, allowing for the efficient cellular response to change.

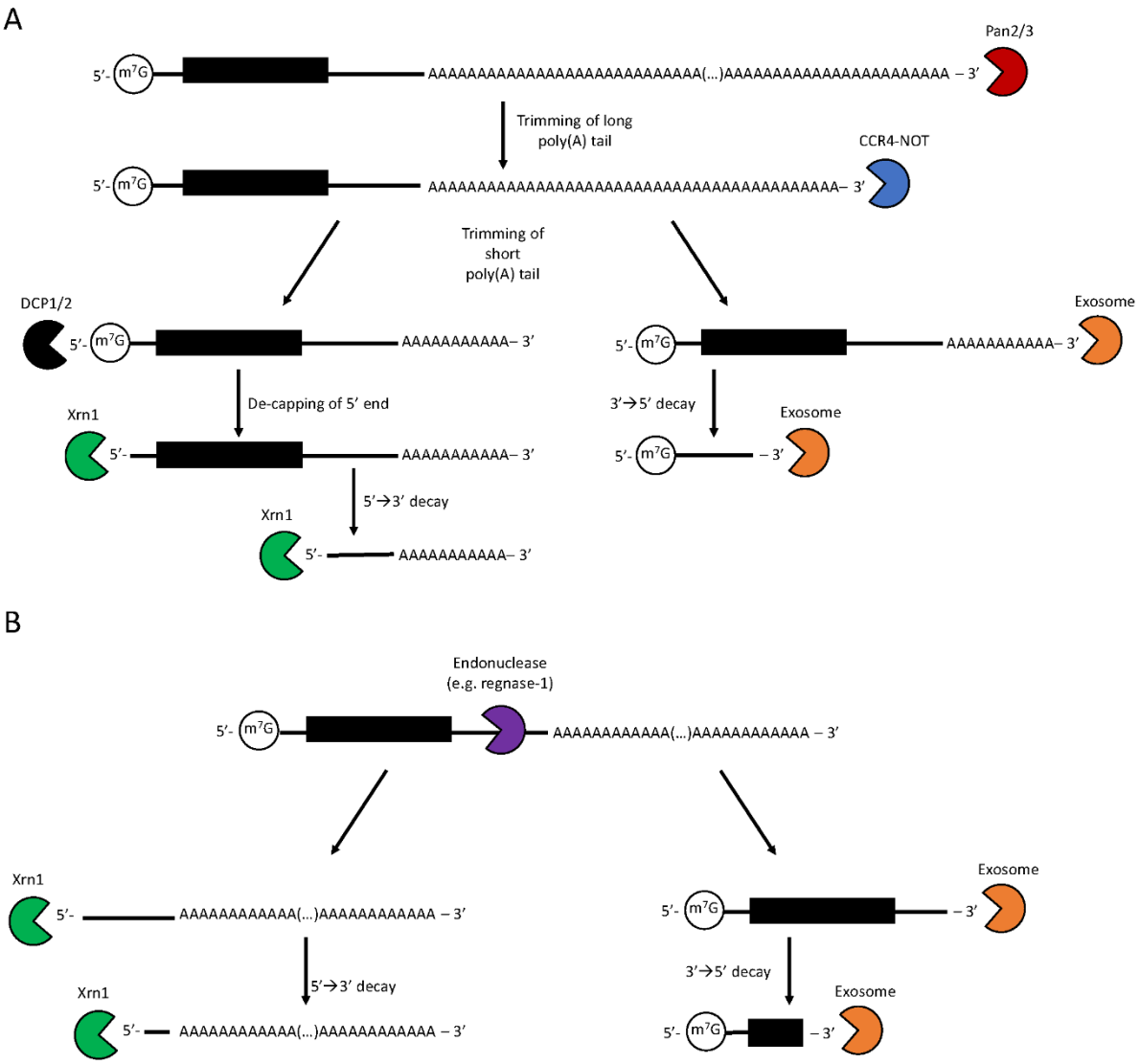

Figure 1: **Canonical deadenylation-dependent and endonuclease-mediated mRNA decay**. (A) Classical decay pathway of poly-(A) mRNAs, where transcripts are deadenylated by PAN2/3 and then CCR4-NOT enzymes. After de-adenylation mRNAs either have the 5’ methylguanosine cap (m^7G) removed by DCP2 followed by degradation by Xrn1 in the 5’-3’ direction, or are degraded by the exosome in the 3’-5’ direction. (B) Endonuclease mediated mRNA decay, where nucleases (e.g. regnase-1) induce the cleavage of transcripts at internal sites, followed by full degradation of transcripts by Xrn1 and the exosome.

1.2 RNA granules

Rather than being degraded, translation of mRNAs can be repressed through the formation of RNA granules (Eulalio et al., 2007, Brengues et al., 2005). These structures are aggregates of RNAs and proteins, where transcripts are held in an untranslated-state; the two most prominent of such structures are processing (P)-bodies and stress granules (SGs). These structures are membraneless cellular compartments which are dynamic – exchanging proteins and RNA continuously with the cytoplasm (Kadersha et al., 2000, Kadersha et al., 2005, Mollet et al., 2008, Andrei et al., 2005).

Thousands of mRNA species localize to P-bodies, highlighting the significance of these regions in controlling the global expression of genes (Wang et al., 2018). In P-bodies, transcripts interact with proteins involved in the deadenylation-dependent decay, miRNA-mediated silencing and nonsense-mediated decay pathways (Kulkarni et al., 2010). Intriguingly, within these structures RNAs can be degraded or sequestered away intact, but inaccessible from the translational machinery (Luo et al., 2018). Immunofluorescent illustration of P-body structure and localization is shown in Figure 2.

On the other hand, stress granules form in response to a stressful stimulus (e.g. viral infection), with phosphorylation of eIF2α leading to arrest of translation (Kedersha et al., 1999). Up to 95% of all transcripts can associate with SGs, illustrating the substantial impact these structures have on the transcriptome (Khong et al., 2017). Untranslated mRNAs accumulate along with small ribosomal subunits, and associate with proteins including poly(A)-binding protein (PABP) and G3BP1 to form SGs (Kedersha et al., 2000, Tourrière et al., 2003). The ability to store RNAs in a non-translating state provides cells with the ability to dynamically regulate gene expression, adding yet another layer of complexity into the control of mRNAs.

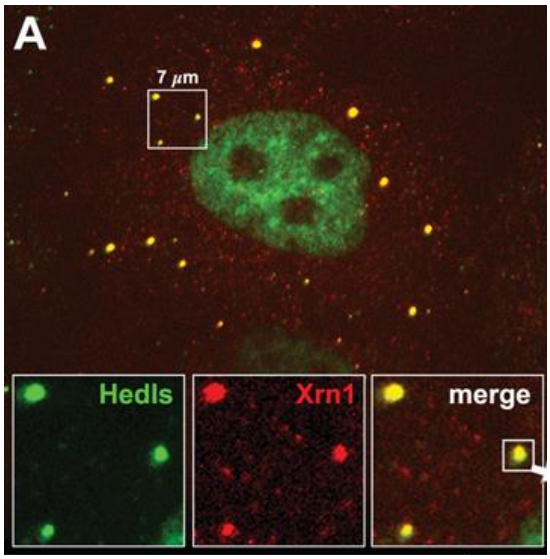

Figure 2**: Immunofluorescent analysis of P-body proteins Hedls (decapping factor) and Xrn1 (exonuclease)** (adapted from Kulkarni et al. 2010).

1.3 RNA binding motifs and post-transcriptional control

In order to regulate RNA, proteins must display a domain that allows them to interact directly with ribonucleotides. These regions are called RNA binding motifs, and they arise in four main forms: RNA recognition motifs (RRMs), zinc fingers (ZFs), double stranded RNA binding motifs (dsRBMs) and KH domains (Cléry & Allain, 2012). The importance of these motifs is evident through their involvement in essential cellular functions – for example, PABP, a key protein involved in translation and mRNA decay, interacts with poly(A) tail by canonical RNA recognition motifs (RRMs) (Deo et al., 1999). RNA binding motifs are also found on proteins that selectively target mRNA subsets. For example, Regnase-1 (MCPIP1), which interacts with mRNAs involved in immune stimulation, binds to target mRNAs via its zinc-finger domains (Garg et al., 2021, Matsushita et al., 2009). Further, within each family of RNA binding motifs there is diversity among targets, varying from protein to protein. For instance, the KH domains of poly-(C) binding protein interact with cytosine-rich ssDNA in telomeres, while the KH domain of splicing factor 1 (SF1) interacts with the branch point sequence (UACUAAC) in pre-mRNA transcripts (Bergland et al., 1997).

RNA binding motifs interact with target RNA sequences via hydrogen-bonding and/or aromatic base stacking (Ding et al., 1999, Teplova & Patel, 2008, Cléry & Allain, 2012, Morozova et al., 2006). Importantly, the composition and structure of these motifs dictate specificity of protein-RNA interactions. For example, RRMs and zinc fingers contain conserved aromatic amino acids which can facilitate interactions with RNA through base stacking between RNA bases and aromatic side chains of amino acids; KH domains, on the other hand, do not engage in base stacking (Ding et al., 1999, Teplova & Patel, 2008, Cléry & Allain, 2012). Structurally, RNA binding motifs can differ greatly from one another. RRMs may extend the

binding surface of their motif to accommodate additional RNA nucleotides to interact; zing fingers can adopt different folding structures to specifically bind RNA; KH domains interact with only 4 nucleotides and have a fixed site of interaction, with specificity determined by small scale differences in orientation of atoms (Conte et al., 2000, Plambeck et al., 2003, Valverde et al., 2008, Du et al., 2007, Braddock et al., 2002). Altogether, a diverse range of RNA binding proteins play key roles in mRNA regulation both specifically, and on a global scale. As more proteins are identified with predicted RNA binding motifs, it is important to understand how these proteins impact RNA regulatory networks.

1.4 Endonuclease-mediated mRNA turnover

All mRNA decay pathways require a ribonuclease to fully degrade transcripts (Muhlrad et al., 1994, Łabno et al. 2016). Exoribonucleases (e.g. Xrn1) degrade transcripts from the ends of the RNA, while endoribonucleases (e.g. Regnase-1) cleave internal sequences often in specific RNAs (Solinger et al., 1999, Muhlrab et al., 1994, Matsushita et al., 2009). Cleavage of transcripts by endonucleases expose unprotected 5' and 3' ends which can then be degraded fully by exonucleases (Eberle et al., 2009). While exoribonucleases are responsible for most RNA decay in cells, it has become apparent in recent years that endonucleases play abundant and diverse roles in regulating gene expression in cells. For example, in miRNA mediated mRNA decay, the catalytic protein Ago2 (argonaut 2) cleaves targeted mRNAs internally, allowing for the regulated and specific repression of thousands of target genes (Ender & Meister, 2010, Alles et al., 2019). In this case, Ago2 is guided by a miRNA that is perfectly complementary to a target mRNA, allowing Ago2 to act as an endonuclease and cleave the transcript. Alternatively, Regnase-1 (MCPIP1, monocyte chemotactic protein-1-induced protein-1) recognizes specific

stem loop structures in transcripts through a zinc finger domain to repress immune system activation (Uehata et al., 2013). Lastly, in nonsense mediated decay, premature stop codons lead to recruitment of the endonuclease Smg6 to the ribosome, which can induce mRNA cleavage (Karousis et al., 2016). As such, Smg6 is a key protein in a quality control mechanism to prevent expression of potentially harmful mRNAs.

While many endonucleases do have sequence specificity, others can cleave only at specific structures of mRNA, or non-specifically. During the immune response, RNaseL (ribonuclease L) cleaves many RNAs non-specifically; however, some mRNAs required for the immune response are able to escape RNaseL cleavage (e.g. interferon-β) and thus permit signalling of the infection to nearby cells (Burke et al., 2019). The presence of target specific endonuclease, and the ability of some transcripts to escape bulk mRNA turnover, allow for the precise regulation of gene expression for subsets of genes in a context specific manner. Thus, endonucleases are key regulatory components in many cellular pathways. With the recent discovery of novel classes of endonucleases domain, it is pressing to discover how these proteins contribute to the already complicated networks of mRNA decay in eukaryotes.

1.5 Regulation of RNAs in the viral immune response

When infected by a virus, multicellular organisms have evolved with ways to limit the spread of the virus between its cells to survive. One essential process in this viral immune response is mRNA repression. To replicate, viruses hijack host machinery, often making use of the ribosomes and structures related to translation for generating proteins (Bushell & Sarnow, 2002). As such, cells have developed mechanisms to shut down translation for most of the transcriptome, while permitting expression of a subset of genes still required to respond to the

infection. Detection of viral RNAs triggers the phosphorylation of eukaryotic initiation factor 2α (eIF2α), which causes the arrest of canonical cap-dependent translation (Novoa et al., 2001). As described earlier, untranslated mRNAs bound to the small ribosomal subunit aggregate in SGs and are unable to be translated (Arimoto et al., 2008, Tourrière et al., 2003). Furthermore, viral RNAs stimulate the activation of RNaseL, an endonuclease which cleaves the majority of viral and cellular RNAs inducing a rapid host cell shut down (Burke et al., 2019). Importantly, specific RNAs involved in the immune response (e.g. interferon-β) are resistant to RNaseL, allowing for specific translation of genes involved in the viral response (Burke et al., 2019).

Upon viral infection, cells release type-I interferons (IFN α/β), signalling to neighbouring cells to respond to the threat (Uehata & Takeuchi, 2020). Type-I interferons cause STAT proteins to dimerize in the cytoplasm and translocate to the nucleus, acting as transcription factors for genes involved in the antiviral and inflammatory responses (Ivashkiv & Donlin, 2014). Targets of this pathway include signalling molecules (e.g. interferons), receptors (e.g. RIG-I), and transcription factors (e.g. STAT1) (Hubel et al., 2019). Overall, during the viral response cells must repress bulk endogenous and viral RNAs, while facilitating expression of genes involved in alerting nearby cells of the viral threat.

To prevent autoimmunity and inflammatory disorder, cells are also able to repress the viral response pathway. Proteins including Regnase-1 (MCPIP1) and Roquin negatively regulate the expression of interferon-stimulated genes through degradation of mRNAs (Takeuchi, 2018). Regnase-1 is highly expressed in immune cells and targets a stem-loop structure in the 3'-untranslated region of mRNAs (Jeltsch et al., 2014). Actively translating mRNAs are targeted at the ribosome by Regnase-1, which acts as an endonuclease cleaving the RNA using its PilT N-terminal RNase-like (PIN) domain. This endonuclease specifically targets genes involved in

immune activation, including *IL-6* and *IL-12b* mRNAs; mice deficient in Regnase-1 develop inflammatory and autoimmune disorders (Takeuchi, 2018, Uehata et al., 2013). Further, Regnase-1 represses expression of HIV proteins dependent on its nuclease domain, illustrating that this nuclease can act as a direct barrier against infection (Liu et al., 2013). Roquin represses a similar subset of mRNAs to Regnase-1, but while Regnase-1 localizes to ribosomes and endoplasmic reticulum, Roquin acts in P-bodies and stress granules (Mino & Takeuchi, 2015). Roquin mediates decay indirectly through a deadenylation dependent mechanism (Takeuchi, 2018). Intriguingly, to cleave RNAs, Regnase-1 must interact with Upf1, a factor required for the NMD pathway, and Roquin-1 acts through interacting with deadenylase CCR4-NOT (Takeuchi, 2018). Thus, although there are many diverse RNA decay pathways, there is redundancy in cells to ensure the tight regulation of specific RNAs.

1.6 NYN domains

N4BP1 YacP-like Nuclease (NYN) domains describe a novel family of proteins predicted to have endonuclease activity (Anantharam & Aravind, 2006). NYN domains are structurally related to PIN and FLAP domains, which are responsible for much of endonuclease mediated mRNA decay in mammalian cells. Common to all these domains is a catalytic core with 4 key aspartic acid residues; these residues coordinate a magnesium/manganese ion for endonuclease activity (Anantharam & Aravind, 2006). In short, this domain and those closely related use aspartic acid residues to chelate a magnesium/manganese ion, which activates water molecules to start a nucleophilic attack on a phosphodiester bond on nearby RNAs, causing a break in the RNA strand (Howard et al., 2015). The importance of PIN and FLAP domains in cellular function is well documented. Both Smg6, a key component of the nonsense mediated decay

pathway, and Regnase-1, an essential regulator of the immune response, make use of PIN domains for exerting their catalytic function (Glavan et al., 2006, Eberle et al., 2009, Yokogawa et al., 2016). XRN1, the protein which conducts the final degradation of most RNAs in the 5'-3' direction, functions through its catalytic FLAP domain (Solinger et al., 1999).

Aravind et al. (2006) identified proteins containing NYN domains across all domains of life (Figure 3), including YacP (bacteria), MJ1085 (archaea), and N4BP1 (eukaryotes). Further, a diverse range of uncharacterized NYN containing proteins in eukaryotes was identified, including N4BP1 paralog KHNYN, PRORP1 (proteinaceous RNase P1), and MARF1 (Meiosis regulator and mRNA stability factor 1). From the current literature, RNA processing roles for many of these proteins have been identified. YacP, a NYN containing protein found in *B. subtilis*, acts as an endonuclease to specifically cleave mRNAs related to the iron uptake response in a translation dependent mechanism (Leroy et al., 2017). Further, YacP appears to show sequence specificity, cleaving most often upstream of lysine (AAA or AAG) codons (Leroy et al., 2017). PRORP1 is a protein specific to *A. thalania* and plays a role in tRNA and mitochondrial mRNA processing (Mao et al., 2016). In mammals, MARF1 is shown to be essential for oogenesis in mice (Su et al., 2012). MARF1 has recently been shown to interact with RNA decay machinery in P-bodies including EDC4, a protein required for efficient decapping of mRNAs. Through its NYN domain, MARF1 directly cleaves targeted mRNAs (Brothers et al., 2020). NYN domains play diverse roles in RNA regulation across species and add further specificity to global RNA decay.

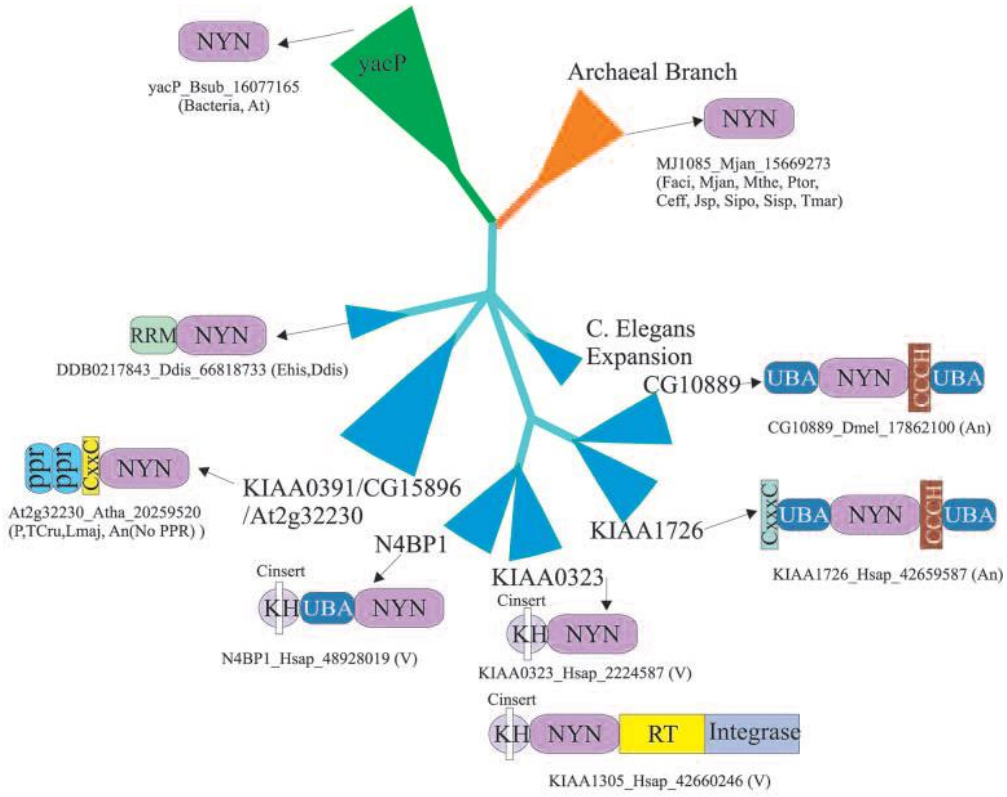

Figure 3: **Phylogenetic tree of NYN domain encoding proteins** (from Anantharam & Aravind, 2006). Proteins have since been characterized as: At2g32230 (PRORP1), KIAA0323 (KHNYN), CG10889 (Regnase-1).

1.7 N4BP1: a novel interferon-stimulated gene with the potential to regulate RNA

While N4BP1 typifies NYN domains, it was originally identified that N4BP1 functions through regulating ubiquitylation. Ubiquitin is a small protein tag which can be added to proteins by coordination of enzymes called E1-E3 ubiquitin ligases. In fact, most often this leads to degradation, as proteins tagged with ubiquitin localize to the proteasome to be broken down. Importantly, ubiquitylation does not always lead to degradation, as the added ubiquitin can be recognized to mediate cell signalling, or serve as a substrate for other modifications (e.g. phosphorylation) (Santonico, 2020). Further, ubiquitylation can regulate the cellular localization of proteins, such as with the oncoprotein Bclb where monoubiquitylation leads to movement from the cell membrane to the cytoplasm (Beverley et al., 2012).

N4BP1 acts as a ubiquitylation buffer, permitting the function of other proteins involved in cancer (Oberst et al., 2007). ITCH is an E3 ubiquitin ligase, which often causes degradation of target proteins including tumour suppressor p73 and oncoprotein c-Jun; N4BP1 competitively inhibits the ubiquitylation of these target proteins by becoming ubiquitinated itself by ITCH, allowing other target proteins to exert their function (Oberst et al., 2007). It was since shown by Sharma et al. (2010) that N4BP1 localizes to the nucleolus, and can be ubiquitinated by Nedd-4, leading to proteasomal degradation (Figure 4). However, SUMOylation (a post-translational modification related to ubiquitylation where SUMO, small-ubiquitin like modifier, is attached to a protein) induces localization of N4BP1 to nuclear foci called promyelocytic (PML) bodies – sites of protein modifications that can be induced by cellular stress (Stadler et al., 1995, Lallemand-Breitenbach et al., 2008). Intriguingly, both the nucleolus and PML bodies have established roles in regulating rRNA and mRNA respectively. Of note, the paper that originally

identified N4BP1 as a nuclear protein used mouse embryonic fibroblasts (Sharma et al., 2010), leaving up to question whether this pattern held true in human cells.

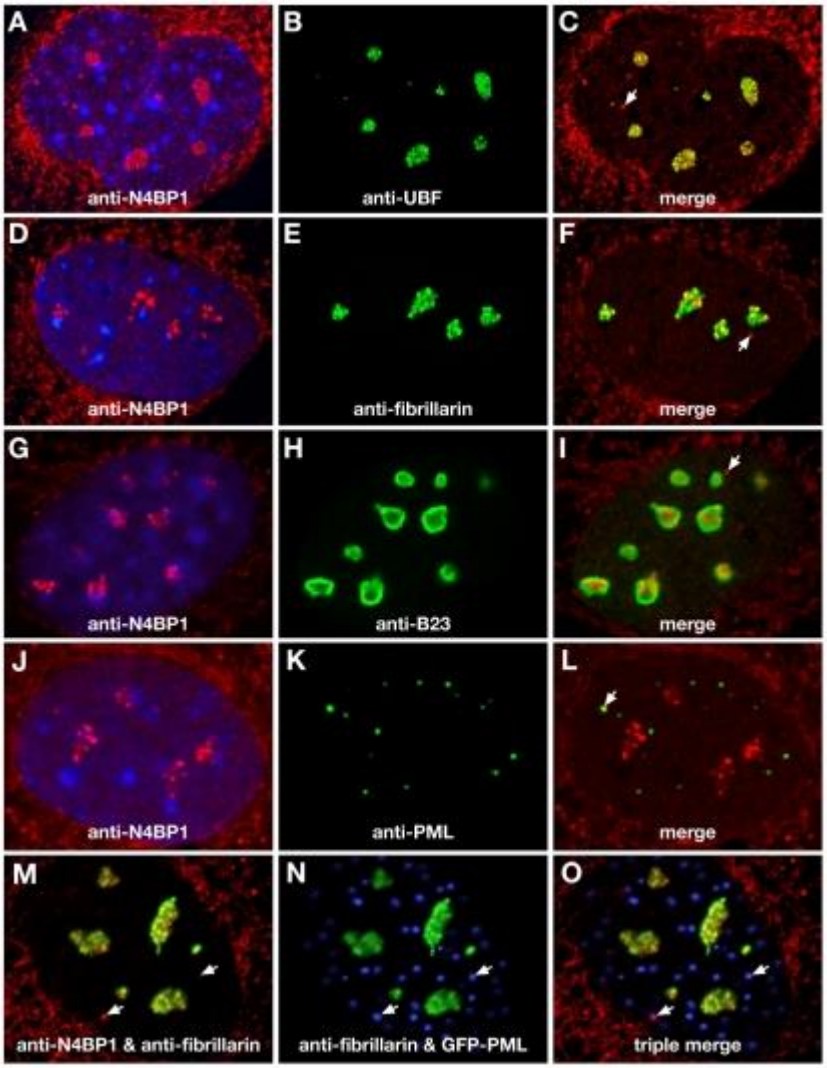

Figure 4: **N4BP1 nuclear localization in MEFs** (from Sharma et al. 2010). Markers of the fibrillar components (UBF and fibrillarin) and granular components (B27) of the nucleolus, as well as PML, a marker of PML nuclear bodies, were used to assess N4BP1 nuclear localization.

Intriguingly, N4BP1 has also been shown to be a regulator of the immune response. Spel et al. (2018) showed that N4BP1 interacts with deubiquitinating enzyme cezanne, which stabilizes a protein TRAF3 (tumour necrosis factor receptor associated factor 3), eventually leading to degradation of NF-κB (nuclear factor κB) and reduced expression of class-I MHC (major histocompatibility complex). Although this work was shown in the context of cancer, it illustrates that N4BP1 can regulate components of the immune system through its role in ubiquitylation. Further, N4BP1 was found to be stimulated by type-I interferon (involved in the viral response) across 10 mammal species, with unknown implications on the immune system (Shaw et al., 2017). Altogether, the literature makes clear that N4BP1 plays an important role in regulating the immune response via ubiquitin interactions in mammals; however, recent work on the RNA regulating role of this protein has highlighted that there is much more to this protein beyond ubiquitylation.

N4BP1 induces decay of viral RNAs. This phenomenon was first shown in fish with N4BP1 repressing grass carp reovirus infection *in vivo* (Cai et al., 2014), but has progressed substantially in the context of human immunodeficiency virus (HIV). Using primary T-cells and macrophage and T-cell lines, Yamasoba et al (2019) illustrated that N4BP1 inhibits HIV replication, and that this occurred through regulating expression of viral mRNAs. Interestingly, N4BP1 overexpression reduced transcript levels for a subset of related RNA viruses including HIV, SIV (simian immunodeficiency virus), MLV (murine leukemia virus) and (human foamy virus), while not others such as Influenza. Along with the potential nuclease NYN domain, this paper identified predicted RNA binding KH domains, strongly suggesting that N4BP1 may play a direct role in interacting directly with RNAs (Figure 5). This interaction was shown by RNA-immunoprecipitation, whereby N4BP1 was isolated from cells following HIV infection, and

quantitative polymerase chain reaction was conducted to examine interacting RNAs. In this assay, numerous HIV mRNAs were isolated solely with N4BP1 mutants with catalytically inactive NYN domains, making clear that N4BP1 interacts with RNA and mediates their decay dependent on its predicted nuclease domain.

Upon T-cell activation, N4BP1 is cleaved by the human paracaspase MALT1 (mucosa-associated lymphoid tissue lymphoma translocation protein 1), limiting the ability of N4BP1 to halt HIV infection (Figure 5, Yamasoba et al., 2019). Such regulation by MALT1 contradicts the idea that N4BP1 enhances the immune response to viruses – MALT1 is activated during the immune response to degrade proteins that act to repress immune activation. For example, PIN domain containing nuclease Regnase-1, which degrades HIV RNAs, also degrades RNAs including *IL-6* and *IL-12b*, both involved in stimulating the immune response. Following activation of T-cells, MALT-1 cleaves Regnase-1 permitting T-cell immune function (Liu et al., 2013). Therefore, the data in Yamasoba et al (2019) propounds the idea that N4BP1 may, limit the immune response, despite its role in cleaving viral RNAs.

The paralog of N4BP1, KHNYN, repressed HIV protein expression, and has high homology with N4BP1 in its RNA binding (KH), nuclease (NYN), and ubiquitin binding (CoCUN/CUBAN) domains (Nepravishta et al., 2019). To repress HIV protein expression, KHNYN interacts with ZAP (zinc finger antiviral protein) in the cytoplasm, and targets CpG dinucleotides on viral transcripts. Further, repression of HIV by KHNYN depends on the presence of both its KH and NYN domains (Ficarelli et al., 2019). ZAP interacts with DDX6, DCP1-DCP2 and XRN1, components of P-bodies which help to fully degrade and repress mRNAs (Goodier et al., 2015). Further, ZAP can localize to stress granules, suggesting that interactions with mRNA decay/repression proteins as a potential mechanism for the full

degradation of HIV mRNA. Intriguingly, N4BP1 was identified in a ZAP interaction screen; the similarity in structure, function (HIV mRNA repression), and the fact that both KHNYN and N4BP1 interact with ZAP illustrate that N4BP1 may have a yet uncharacterized cellular role in RNA regulation via ZAP (Ficarelli et al., 2019). Further, N4BP1 has also recently been identified in a biotinylation-ID screen to be in proximity with DCP1 (Youn et al., 2018), a protein cofactor for mRNA decapping frequently found in P-bodies. These findings suggest that N4BP1 may have yet uncharacterized roles in the cytoplasm through interactions with RNA binding proteins.

In recent years some light has been shed on how N4BP1 regulates the mammalian immune response. Caspase-8 is a protease that cleaves proteins to mediate immune activation, similarly to MALT1 – upon activation, caspase-8 potently cleaves and inactivates N4BP1 (Figure 5, Gitlin et al., 2020). Intriguingly, caspase-8 is a cytoplasmic protein, and cell fractionation experiments in human HEK293T (human embryonic kidney 293T, herein referred to as 293T) cell line illustrate that N4BP1 is predominantly cytoplasmic as well, highlighting a novel and previously uncharacterized role of N4BP1 outside of the nucleus. While activation of some immune toll-like receptors (TLR3,4) induces Caspase-8 activation through TRIF adapter protein, others including TLR1/2, TLR7, and TLR9 operate independently of TRIF. As such, only in TRIF-caspase-8 independent pathways, N4BP1 remains intact, and was shown to repress the expression of various cytokines (e.g. IL-6, TNF – tumour necrosis factor) and chemokines (CXCL1) both in primary human macrophages and *in vivo* using a mouse model.

Most interestingly from this paper, RNA sequencing from human bone marrow derived macrophages for both N4BP1 wild-type and knock-out samples illustrated that N4BP1 mediates repression of the translation of many mRNAs involved in the immune response (including IL-6, and TNF). While RNA-immunoprecipitation showed that N4BP1 directly interacts with HIV

RNAs, RNA sequencing data did not indicate whether N4BP1 directly degrades the identified RNAs, or whether RNA decay occurs indirectly through the interactions with other proteins (Yamasoba et al., 2019, Gitlin et al., 2020). In 2021, a paper was published offering a possible explanation, showing that N4BP1 negatively regulates NF-κB via interactions with NEMO (NF-κB essential modulator; Shi et al., 2021). In this way, N4BP1 mediated repression of NF-κB target genes (including IL-6 and TNF) independent of N4BP1 nuclease activity. Altogether, N4BP1 is a potent regulator of the immune response through repressing the translation of specific viral and endogenous RNAs and is cleaved during the immune response by both MALT1 and Caspase-8.

Both MALT1 and Caspase-8 cleave repressor proteins in order to activate the immune system; cleavage sites of both proteins are in close proximity (R509 and D488 respectively) residing in the linker region of N4BP1 between KH and NYN domains (Figure 5), strongly implicating N4BP1 as a negative regulator of the immune response (Yamasoba et al., 2019, Gitlin et al., 2020). Moreover, the related roles of MALT1 and Caspase-8 on regulating N4BP1 may offer further specificity into overall yet uncharacterized RNA regulating pathways.

N4BP1 has been reported to negatively regulate the immune response, and restrict viral (HIV) infection. Similarly, Regnase-1 holds many similarities to N4BP1 – both of these nucleases contain related catalytic domains (NYN and PIN respectively), are interferon induced, inhibit immune cell activation (both repress expression of mRNAs including IL-6) and are cleaved by MALT1. Further, both proteins repress the expression of HIV proteins dependent on their nuclease domains. The presence of these two proteins may show a form of redundancy, or simply offer related yet distinct pathways to fine-tune RNA regulation during the immune response. A possible explanation of the impact of these proteins is that they may both limit

inappropriate immune responses and act as a first barrier against viral infection (as nucleases). However, once the virus has been recognized and activates the immune system, it is most beneficial for cells to degrade N4BP1 and Regnase-1.

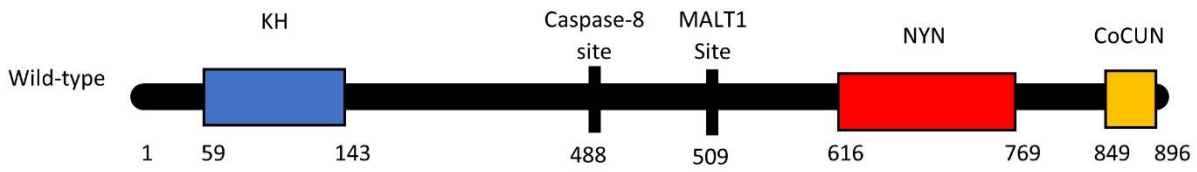

Figure 5 : **Schematic representation of N4BP1**. Depicted are domains predicted to have RNA binding (KH) and nuclease (NYN) activity, as well as established ubiquitin binding domain CoCUN (cousin of cullin-binding domain associated with NEDD8) and protease cleavage sites.

1.8 Rationale and hypothesis

The mechanism through which N4BP1 acts in endogenous mRNA degradation, what dictates its localization, and how it functions in different regions of the cell are largely unknown. To fill in these substantial gaps in the literature, my project aimed to 1) assess whether N4BP1 can post-transcriptionally repress gene expression of targeted mRNA, 2) determine where N4BP1 localizes in human cells, and whether this is dictated by its domain architecture and 3) identify N4BP1-interacting proteins across multiple cell lines. ***I hypothesize that N4BP1 degrades RNAs in human cells, and that its activity and localization are regulated by its interaction with protein(s) that localize to P-bodies.***

Methods

Cell fractionation

HeLa (Henrietta Lacks) or U-2 OS (human both osteosarcoma epithelial) cells were seeded in a 6-well plate at 25% confluency, and transfected with 2µg of FLAG-N4BP1. Cells were washed with 1mL of PBS (phosphate buffered saline), lifted using 0.5mL of 0.25% trypsin-EDTA, resuspended in an additional 0.5mL PBS and transferred to 1.5mL Eppendorf tubes. Samples were centrifuged at 1200 rpm for 2 minutes, supernatant was aspirated, and cells were resuspended in 500µL of PBS, centrifuged at 8000 rpm for 1 minute, and supernatant removed to leave only 20µL. Next, 450µL of lysis buffer (0.1% NP40 in PBS) was added to the sample, cells were resuspended by pipetting up and down five times, and 150µL of this lysate was transferred to a tube labelled “whole cell fraction”. Remaining lysate was spun down at 8000 rpm for 10 seconds, and 150µL of the supernatant was added to a new tube labelled “cytosolic fraction”. Remaining supernatant was removed, and the pellet (labelled "nuclear fraction") was resuspended in 500µL of lysis buffer, centrifuged at 8000 rpm for 10 seconds, supernatant discarded, and resuspended in 90µL of 1X Laemmli in lysis buffer. Finally, 30µL of 6X Laemmli was added to whole cell and cytosolic fractions, along with 1µL of benzonase (Millipore) to every tube. Samples were heated at 95°C for 10 minutes, then run on a 9% acrylamide gel for 1.5 hours, transferred overnight at 30V at 4°C onto a nitrocellulose membrane, followed by 1 hour of blocking in 5% skim milk. Membranes were blotted for primary antibodies for 2 hours at room temperature. Primary antibodies were diluted 1:1000 (mouse anti-FLAG), 1:20000 (mouse anti-GAPDH) or 1:15000 (mouse anti-hnRNP), in in TBST (Tris-buffered saline with 0.1% tween20) with 4% BSA (bovine serum albumin) and 0.04% sodium azide. Primary antibodies were recovered, and membranes were washed 3 times

with TBST, and incubated in appropriate secondary antibody conjugated to horseradish peroxidase diluted 1:1000 in 5% skim milk for 1 hour at room temperature. Blots were imaged using Imagequant LAS 4000.

Immunofluorescence

HeLa cells were plated on glass coverslips in 24-well plates at 25% confluency, and transfected 24 hours post-plating. Cells were transfected with 100µL of Opti-MEM media (Invitrogen) and 5µL of PEI (Polyscience), along with 250ng of plasmid DNA containing either FLAG-N4BP1 WT or mutants either alone or with V5-EDC4, along with non-transfected controls. All subsequent incubations were carried out at room temperature (RT). At 24 hours post-transfection, media was removed and cells were fixed in a fume hood using 4% paraformaldehyde in PBS for 20 minutes. Slides were then washed four times with 500µL of PBS, and then permeabilized using 300µL of 0.1% TritonX100 in PBS for 15 minutes. Next, cells were washed twice with PBS as above, and blocking was carried out using 300µL 4% bovine serum albumin in PBS for 30 minutes. Primary antibodies (mouse anti-FLAG, rabbit anti-V5, rabbit anti EDC4, rabbit anti-DCP1) were added in a dilution of 1:500 in 4% BSA to make up a final volume of 250µL and incubated with slips for 1 hour.

The remaining steps were carried out in the dark. Wells were washed with PBS 4 times as above, and then incubated in the dark with 1:500 dilutions of secondary antibodies (Alexa Fluor 488 rabbit and Alexa Fluor 594 mouse) in 4% BSA, making a final volume of 250µL for 1 hour. Cells were washed 4 times with PBS as above, and then incubated with 500µL of 300nM DAPI for 10 minutes. Final washing was carried out 4 times with PBS. One drop of Prolong Gold

mounting media (Invitrogen) was placed on a glass slide, and coverslips were lifted using forceps and carefully flipped upside down onto the mounting media. Slides were then incubated in the dark at 4°C for 1-7 days before imaging. Imaging was carried out using the Zeiss LSM 800 Airyscan Confocal Microscope.

Co-immunoprecipitation

293T cells were seeded into a 10cm culture plate at 25% confluency, and transfected with plasmid DNA (3µg FLAG-N4BP1, 2µg FLAG-MARF1, 750ng GFP, 3µg V5-EDC4), 2mL of Opti-MEM and 55µL of polyethylenimine (PEI) at 24 hours post-seeding. Cells were harvested 24 hours post-transfection. Cell pellets were then lysed by resuspending in a lysis buffer (50 mM HEPES–NaOH pH 7.5, 100 mM KCl, 2 mM EDTA, 0.1% NP40 and 10% glycerol) with addition of 1mM DTT (Bioshop), 1X protease inhibitor cocktail (PIC, Sigma), 1X PMSF (Bioshop), and 1µL of benzonase (Millipore) per sample. Cell suspensions were pipetted up and down 20 times and kept on ice for 20 minutes. Lysate was spun down at 13000 rpm at 4°C for 15 minutes and transferred into a new tube. A Bradford assay was performed to quantify protein concentrations, and 2mg of total protein was added to make up 1mL of lysis buffer. For use in the later western blot, 30µL of lysate (herein "input") was taken into a separate tube, and an equal volume of 2X Laemmli buffer was added. Input samples were stored at -20°C. Remaining lysates were then pre-cleared by incubating with 30µL of protein-G agarose beads (Millipore) at 4°C while rotating for 45 minutes. Samples were spun down at 4000 rpm for 1 minute, and lysate was transferred to new tubes. Next, 20µL of FLAG-M2/protein-G agarose beads (Sigma) were added to the lysates, and samples were incubated at 4°C while rotating overnight. Lysates were then centrifuged at 4000 rpm for 1 minute and the remaining liquid was discarded from each

sample. The beads were washed five times with lysis buffer, spinning down each time as above. Remaining buffer was removed to leave a final volume of 30μL, and an equal volume of 2X Laemmli buffer was added to each tube. Samples were boiled at 95°C for 10 minutes, and then assessed by western blotting as described above.

Mass spectrometry

Lentivirus encoding N4BP1-V5 was generated by transfecting pLENTI-6 or pLEX plasmids designed to express N4BP1, along with psPAX and VSVG packaging plasmids into 293T cells at 40% confluence in a 10cm petri dish. After 24 hours, media was removed and replaced with fresh DMEM media; at 48 hours post transfection media was collected in a 10mL syringe, passed through a 45μm filter and stored in cryotubes at -80°C. For infection of U-2 OS and HeLa cells, a 6-well plate of cells at 50% confluence had media replaced with 1mL of virus media (virus for U-2 OS cells generated with pLENTI6 vector; virus for HeLa cells generated with pLEX vector), along with 1μL of polybrene and 1mL of cell culture media (DMEM and McCoy's for HeLa and U-2 OS, respectively). At 24 hours post infection, media was removed and replaced again with virus media, polybrene and standard culturing media. At 48 hours post-infection media was removed and replaced with 2mL of standard culture media, and at 72 hours post-infection, cells were selected for infection by adding blastocidin (5μg/mL for pLENTI6) or puromycin (2μg/mL, for pLEX). A control well was kept with cells uninfected by the virus - both the infected and control well were incubated with antibiotic until all cells in the control well had died, and the media for the infected cells was then replaced with culturing media to allow cells to recover. Expression of N4BP1 was assessed by blotting cell lysates for V5.

After expression was confirmed, stably expressing N4BP1-V5 cells, as well as uninfected control cells were cultured in triplicate in 15cm dishes. At confluence cells were lifted, lysed and pre-cleared as described in the co-immunoprecipitation above. Of note, while the buffer for U-2 OS analysis was the same as that used above in co-immunoprecipitation assays, the buffer for mass spectrometry experimentation with HeLa cells was composed as follows: 50mM Tris-HCl (pH 7.5), 150mM NaCl, 0.5% NP-40, 2mM EDTA, 1mM DTT, PIC (1X), PMSF (1X), and 1μL of benzonase per sample. Inputs of 2% total lysate volume were collected at this point, and the remaining lysate was incubated with rabbit anti-V5 antibody overnight at 4°C (1μL antibody/mg protein). The following morning, 40μL of protein-G agarose beads was added to the immunoprecipitated samples and incubated at RT for 2 hours. Samples were then spun at 1200 rpm for 1 minute, and 2% of the volume was taken (herein labelled as "supernatant"). Remaining liquid was removed from the beads, and the beads were washed 4 more times by adding 1mL of lysis buffer, spinning at 1200 rpm for 1 min, and then removing the solution. Western blotting was performed on input and supernatant of samples to assess the efficiency of immunoprecipitation (V5 antibody) and lack of contamination (by blotting for actin). Washed beads were sent to the proteomics facility in the Lady Davis Institute.

Dual luciferase assay

293T cells were plated in 6-well plates at 25% confluency and transfected 24 hour post-seeding. Transfections were set up with 0.5mL of Opti-MEM, 10μL of PEI, and plasmids of LNHA - N4BP1 (2ug either WT, D623N or ΔNYN) or LacZ (500ng). To all transfections 20ng was added of separate plasmids encoding Renilla luciferase – 5BoxB and Firefly luciferase. Cells were washed with 1mL of PBS, lifted using 0.5mL of 0.25% trypsin-EDTA, resuspended in an

additional 0.5mL PBS and transferred to 1.5mL Eppendorf tubes. Tubes were centrifuged for 2 minutes at 5000 rpm, and supernatant was removed. Cells were resuspended in 90µL of passive lysis buffer (Promega), vortexed briefly, and incubated on ice for 20 minutes, with vortexing every few minutes. Samples were then spun down at maximum speed for 15 minutes at 4°C, and supernatant was transferred to a fresh tube. Next, 5µL of each sample was added to 2 new tubes for technical replicates. For each replicate, we first measured the expression of the firefly luciferase as an internal control by adding 20µL of Promega's proprietary firefly luciferase substrate and taking luminescent measurements with a Glomax 20/20 luminometer (Promega). Then 20µL of the Renilla luciferase substrate was added to the sample and the luminescence was measured again using the luminometer. The ratio of Renilla luciferase luminescence to Firefly luciferase luminescence was calculated and averaged across technical replicates before being expressed as a percentage of the control LacZ.

Quantitative polymerase chain reaction (qPCR)

Isolation of RNA for qPCR assays was performed using the total RNA mini-kit (Biobasic). All samples containing RNA were kept on ice, and centrifugation was carried out at 4°C. In short, a confluent 6-well plate of 293T cells were pelleted, resuspended in 450µL of RLT buffer, passed through a 26-gauge needle six times, and then vortexed. Next, 225µL of 100% ethanol was added, and the solution was mixed by pipetting 20 times, and then loaded onto EZ-10 silica membrane spin columns. Samples were centrifuged at 12000 $\times$ g for 1 minute, washed with 500uL of RW buffer, spun once more for 30 seconds, washed with 500µL of buffer RPE and spun again. After discarding of the flow-through, the samples were centrifuged again to remove any residual buffer. The RNA was eluted in 44µL of nuclease free water and incubated at 50°C

for 2 minutes before being spun down for 1 minute in a clean collection tube. To prevent DNA contamination, RNA samples were treated with 1µL of Turbo DNase (Invitrogen) along with adding 5µL of Turbo DNase buffer and incubated at 37°C for 1 hour. To stop the reaction 6µL of DNase inactivation reagent was added, the samples vortexed, and then incubated at RT for 7 minutes. RNA was then isolated by centrifuging at $10000 \times g$ for 2 minutes.

To generate cDNA (complementary DNA), RNA samples were reverse transcribed as follows using a kit from Thermo Scientific: 500ng of RNA was added to water and 0.5µL of 100µM random hexamer primers to make up a final volume of 6.25µL, heated to 65°C for 5 minutes and then quickly cooled to 4°C. Subsequently, 2µL of 5X reverse-transcription buffer, 0.5µL of 10mM dNTPs, 0.25µL of RNase inhibitor, and 0.5µL of Maxima RT enzyme were added to samples. This final solution was heated at 50°C for 30 minutes, 85°C for 5 minutes, and then removed and diluted in 20µL of water.

To set up qPCR, 2µL reactions made as follows: 12.5µL of 2X GoTaq qPCR Master Mix (Promega), 1µL of primer mix (10µM of forward and reverse primers), 5µL cDNA and water to make up to 25µL. Samples were mixed by vortexing, then 10µL of each sample was loaded in duplicate (technical replicates) into twin.tec Real-Time qPCR 96-well plates (Eppendorf). Using the Mastercycler Pro machine (Eppendorf) samples were treated as follows: 95°C for 3 minutes, and then 40 cycles of (95°C for 15 seconds, 55°C for 15 seconds, 58°C for 20 seconds).

Transfection procedure

Plasmid transfections using HeLa and 293T cells were carried out by adding PEI reagent from Polyscience (5μL for 24-well plate, 10μL for 6-well plate) and optiMEM media from Invitrogen (100μL for 24-well plate, 500μL for 6-well plate) to plasmid DNA, vortexed for 10 seconds, then incubated at RT before adding to plated cells at 50% confluence. Cells were incubated with the transfection reagent for 24 hours prior to use.

For transfecting U2-OS cells, Lipofectamine 2000 from Invitrogen (1μL for 24-well plate, 2μL for 6-well plate) was added to optiMEM media (50μL for 24-well plate, 250μL for 6-well plate) and plasmid DNA was mixed with the equal volume of optiMEM media, and the two mixtures were incubated at RT for 10 min. The lipofectamine and plasmid solutions were then mixed and vortexed for 10 seconds, then added to cells at 50% confluence. After 6 hours the media was removed from cells and replaced with fresh McCoy's media. Cells were then cultured overnight prior to use.

Cell lines

All cell lines were incubated at 37°C and 5% CO_2 in culture media containing 5% fetal bovine serum and 1% penicillin-streptomycin. HeLa, 293T and U-2 OS cells were from American Type Culture Collection (CCL-2, CRL-3216, and HTB-96, respectively). HeLa and cells were cultured with DMEM media (Wisent), whereas U-2 OS cells were cultured using McCoy's media (Wisent).

Antibodies

Primary antibody for M2-FLAG (F1804-200UG) was obtained from Sigma, while V5 (13202S) and actin (4967S) antibodies were from Cell Signalling. For immunofluorescent analysis, the EDC4 (A300-745A-M) and DCP1 (A303-590A) antibodies were from Bethyl, and the secondary antibodies Alexa Fluor 488-rabbit (A-11034) and Alexa Fluor 594-mouse (A-11032) were from Life Technologies. The HA (901514) antibody was obtained from Bio-Legend. Used in cell fractionation experiments, GAPDH antibody (365062) was from Santa Cruz Biotechnology, and hnRNP antibody (100-672) from Novusbio.

DNA constructs

Full-length N4BP1 was amplified from a pcDNA 3.1 vector (a gift from the lab of Christopher Overall) and cloned into the EcoR1 and Not1 sites of the pCI-λNHA vector. N4BP1-V5 was generated by gateway cloning of pDONR-N4BP1 into pLENTI6 and pLEX plasmids. Mutants and N4BP1 fragments were generated by quick-change mutagenesis using Phusion Hot-Start II polymerase. The pCI-λNHA-LacZ and reporter plasmids (RL-5BoxB and FL) are described previously (Zipprich et al., 2009). All plasmids were originally obtained from Addgene.

Primers

qPCR primers for Renilla-luciferase reporter:

5’- GAATTTGCAGCATATCTTGAACCAT -3’

5’- GGATTTCACGAGGCCATGATAA -3’

qPCR primers for Firefly-luciferase reporter:

5’- CCTTCGATAGGGACAAGACAA -3’

5’- AATCTCACGCAGGCAGTTCT -3’

Cloning N4BP1 into pCI-LNHA:

5’- AGCTCAGTGAATTCGCGGCCCGGGCGGTGCTGGACGAGTTC -3’

5’- TCTAGACTCGAGCGGCCGCTTATTTTTCGAACTGCGGGTGGC -3’

Cloning N4BP1 into pDONR:

5’- GGGGACAAGTTTGTACAAAAAAGCAGGCTACCATGGCGGCCCGGGCG GTGCTG -3’

5’- GGGGACCACTTTGTACAAGAAAGCTGGGTCTTTTTCGAACTGCGGGTG GCT -3’

Making D623N mutation:

5’- AAACACATTGTTATAAATGGGAGCAATGTTGCAATTACCC -3’

5’- GCAACATTGCTCCCATTTATAACAATGTGTTTCAAATCCG -3’

Making ΔNYN mutation:

5’- AAAAAATGAACCAGGGAGAACGGATGAGTTTCTTCAGAAGGAAGT -3’

5’- GACAGACTTCCTTCTGAAGAAACTCATCCGTTCTCCCTGGTTCAT -3’

Generation of N4BP1 fragment 1 (2-296):

5’- CACCCGTGGGATCCGCGGCCCGGGCGGTGCTGGACGAGTTC -3’

5’- CACCCGTGGTCGACTTACTTCGTATGCCTTTCTTCAGAATC -3’

Generation of N4BP1 fragment 2 (268-601):

5’- CACCCGTGGGATCCGGTCTAACCCCAGATGAAGAGGCA -3’

CACCCGTGGTCGACTTATTTTAGAGTATCTCGAAACCTTTG -3’

Generation of N4BP1 fragment 3 (575-896):

5’- CACCCGTGGGATCCACTGATGCAAGGTCGGCAGGACCT -3’

5’- CACCCGTGGTCGACTTATTTTTCGAACTGCGGGTGGC -3’

Results

3.1 Tethering of N4BP1 to a reporter mRNA inhibits protein synthesis.

N4BP1 contains a NYN domain that has been proposed to have nuclease activity (Yamasoba et al., 2019). In addition, it has been shown to repress viral RNAs (*tat*/*rev*, *vif* and *gag*) in a NYN-dependent manner (Yamasoba et al., 2019). Supporting the notion that N4BP1 can act as a nuclease, a point mutation to an aspartic acid residue in the proposed catalytic core of this NYN domain (D623N) ablated NYN-mediated viral RNA silencing. Gitlin et al. proposed that N4BP1 may repress endogenous mRNAs involved in the mammalian viral response (Gitlin et al., 2020). However, whether N4BP1 can silence target RNAs independent of its mode of recruitment, and whether the NYN domain plays a role in the silencing, has yet to be established.

To assess the ability of N4BP1 to repress mRNA expression, a well-established λN-BoxB tethering system (Bos et al., 2016) was utilized to recruit ectopic N4BP1 to a reporter mRNA. In short, 293T cells were co-transfected with plasmids encoding a *Renilla* luciferase (RL) reporter with 5-BoxB stemloop elements in its 3' untranslated region, and either λNHA-LacZ (a negative control), wild-type λNHA-N4BP1 or a number of N4BP1 mutants. In this assay wild-type (WT), as well as mutant N4BP1 mutants D623N (NYN point mutant identified in Yamasoba et al., 2019), and ΔNYN (NYN deleted) were generated with a λNHA tag (Figure 6). Cells were also transfected with a plasmid encoding *Firefly*-luciferase (FL) for normalizing transfection efficiency. In this system, the λN tag on the fusion protein has a high affinity to BoxB stemloops in mRNA, and thus co-expressed λNHA-N4BP1 will be recruited to the RL-5BoxB 3' untranslated region (Figure 7A). Cells were isolated 24 hours post-transfection in order to measure luciferase activity (B) and assess ectopic protein expression (D). Total RNA was also

isolated to measure reporter mRNA levels by quantitative reverse transcription PCR (RT-qPCR) (C). Luciferase assay data demonstrated that wild-type λNHA-N4BP1 efficiently repressed the expression of the RL-5BoxB reporter mRNA as compared to the LacZ control. Wild-type N4BP1 repressed the tethered RL reporter expression to a level of 6.9% ($p = 1.9E-8$), while D623N repressed to a level of 27.4% ($p = 9.1E-5$) and ΔNYN to 60.1% ($p = 3.9E-5$) (Figure 7B). When normalizing values to ΔNYN rather than LacZ, significant values were found for both WT (11.4%, $p = 1.5E-5$) and D623N (45.5%, $p = 2.8E-3$). Lastly, the WT samples differed significantly when normalized to the D623N mutant (25.1%, $p = 0.0113$). Significant differences were set as $*p < 0.05$, and p-values were generated using an unpaired two-tailed Student's T-test.

Measuring luminescence was used to assess the protein expression of RL, which could be impacted by N4BP1 at the level of protein (e.g. post-translational modifications) or RNA (e.g. sequestering in P-bodies, endonuclease-mediated cleavage). To determine whether N4BP1 impacted the steady-state levels of RL mRNA, RT-qPCR was performed on the samples outlined above. A fraction of cells isolated 24 hours post-transfection were lysed and total RNA was isolated. Following DNaseI treatment, RNA was then reverse transcribed, and cDNA generated was analyzed by qPCR using gene-specific primer pairs for RL and FL. Figure 7C illustrates that WT N4BP1 tethering to an mRNA reporter led to a decrease in the steady-state levels of RL-5BoxB mRNA (17.3%) ($p = 1.14E-6$) as compared to a LacZ control. Further, both the D623N mutant (17.2%, $p = 4.37E-7$) and ΔNYN mutant (37.1%, $p = 1.25E-4$) significantly differed from LacZ. Intriguingly, the point mutant D623N ($p = 0.95$) did not significantly differ from the repression shown by the WT, while ΔNYN N4BP1 had roughly double the level of reporter

mRNA of the WT ($p = 1.30E-2$). Overall, this data suggest that N4BP1 promotes the decay of reporter mRNA when artificially tethered to it, and this decay is dependent on its NYN domain.

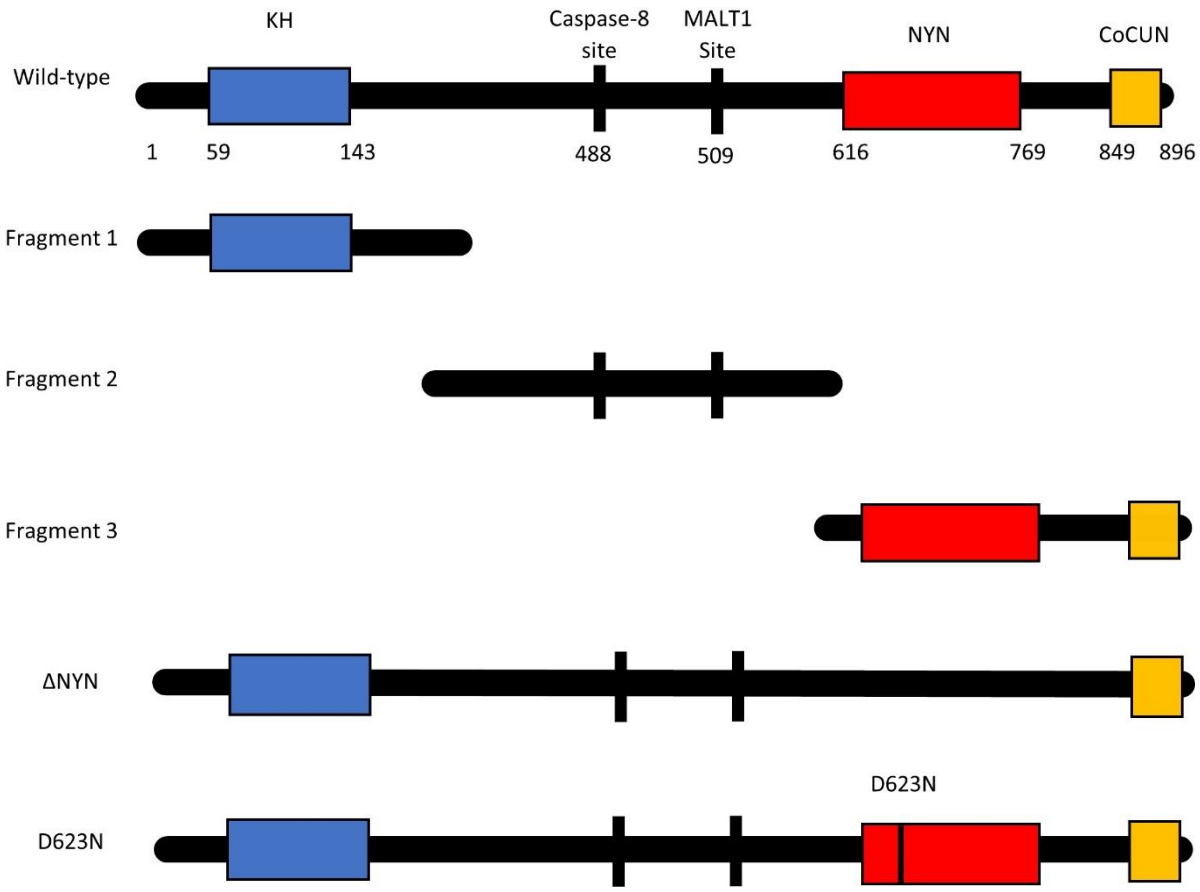

Figure 6: **N4BP1 WT and mutant protein annotation.** Schematic representation of N4BP1 and mutants generated for experimentation. The KH domain has predicted RNA binding capacity, the NYN domain has predicted nuclease activity, and the CoCUN domain is a ubiquitin binding domain. Cleavage sites for MALT1 and Caspase-8 are illustrated in the central linker region of the protein.

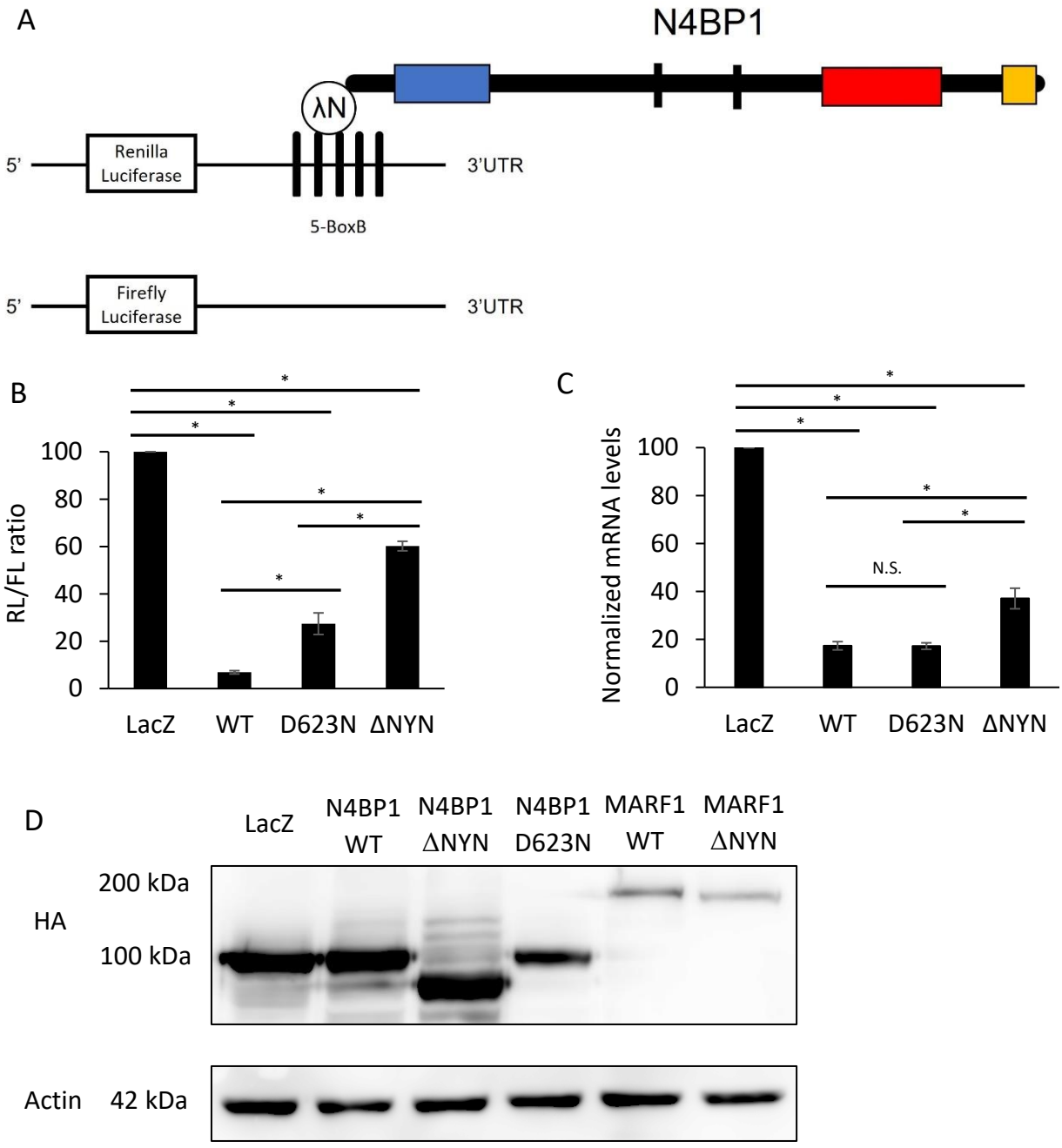

Figure 7: **N4BP1 represses a tethered mRNA reporter, while D623N and ΔNYN mutations cause de-repression. (**A) Schematic representation of *Renilla* luciferase (RL)-encoding mRNA reporter, containing five 19-nt BoxB structural elements, interacting with **λ**NHA-tagged N4BP1, as well as a *Firefly* luciferase (FL)-encoding mRNA. (B) RL activity detected in lysates from 293T cells expressing the indicated protein, measured using a luminometer. Cells were co-transfected with plasmids expressing RL-5BoxB reporter, FL, and indicated tethered proteins. The chart represents normalized mean values of RL luminescence from 3 experiments. RL activity while tethered to **λ**NHA-LacZ was set as 100. (C) RL mRNA levels detected in lysates of 293T cells expressing the indicated proteins., measured using RT-qPCR. Cells were co-

transfected with plasmids expressing RL-5BoxB reporter, FL, and indicated tethered proteins as above. The chart represents the mean value of RL mRNA from 3 experiments. RL mRNA level while tethered to λNHA-LacZ was set as 100 (D) Western blot analysis for LacZ, and WT and mutant forms of N4BP1 and MARF1 used in Figures 7-8. Error bars represent SEM from multiple independent experiments. P-values were calculated using an unpaired two-tailed Student's T-test. *$p < 0.05$. N.S. = non-significant.

While my data suggest that tethering N4BP1 can efficiently repress a targeted mRNA in a NYN-dependent manner, we wished to compare its silencing activity to that of another NYN-containing protein that has characterized endonuclease activity, MARF1 (meiosis regulator and mRNA stability factor 1) (Brothers et al., 2020). To this end, luciferase and RT-qPCR assays were performed as above on 293T cells co-transfected with plasmids encoding RL-5BoxB, FL, and either the WT or ΔNYN variants of λNHA-N4BP1 and λNHA-MARF1 (protein expression illustrated in Figure 7D, domain architecture of MARF1 in Figure 8A). Since the ΔNYN mutation, but not D623N inhibited N4BP1 mediated mRNA decay as shown above (Figure 7C), the ΔNYN mutant was used for comparison. Luciferase assays demonstrate that wild-type N4BP1 represses RL-5BoxB to similar levels as compared to MARF1, while deleting the NYN domain from each lead to a similar level impaired repression (Figure 8B). Similarly, RT-qPCR data (Figure 8C) illustrates that N4BP1 and MARF1 decrease RL-5BoxB mRNA steady-state levels to a similar degree, and both do so in a NYN-dependent manner. However, ΔNYN mutants for both N4BP1 and MARF1 did not induce de-repression to the level of the LacZ control, suggesting that there may be a mix of mRNA decay and translational repression carried out by these proteins. Therefore, N4BP1 induces NYN domain dependent mRNA decay of tethered mRNAs in cells to similar levels of MARF1, a putative NYN dependent endonuclease.

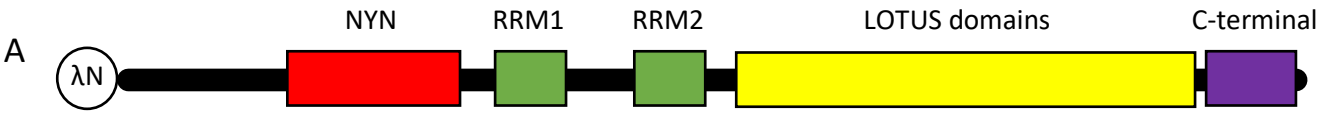
A
NYN
RRM1
RRM2
LOTUS domains
C-terminal
λN

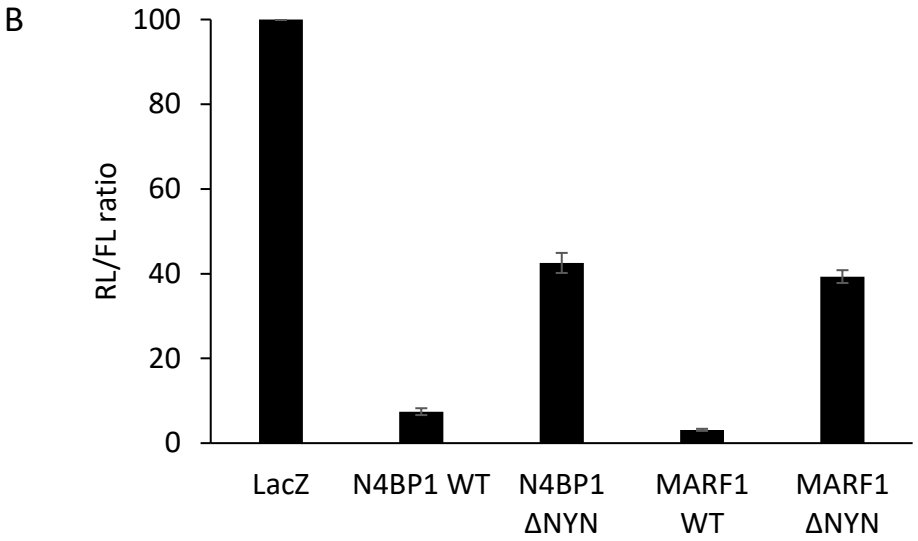
B
RL/FL ratio
100
80
60
40
20
0
LacZ
N4BP1 WT
N4BP1 ΔNYN
MARF1 WT
MARF1 ΔNYN

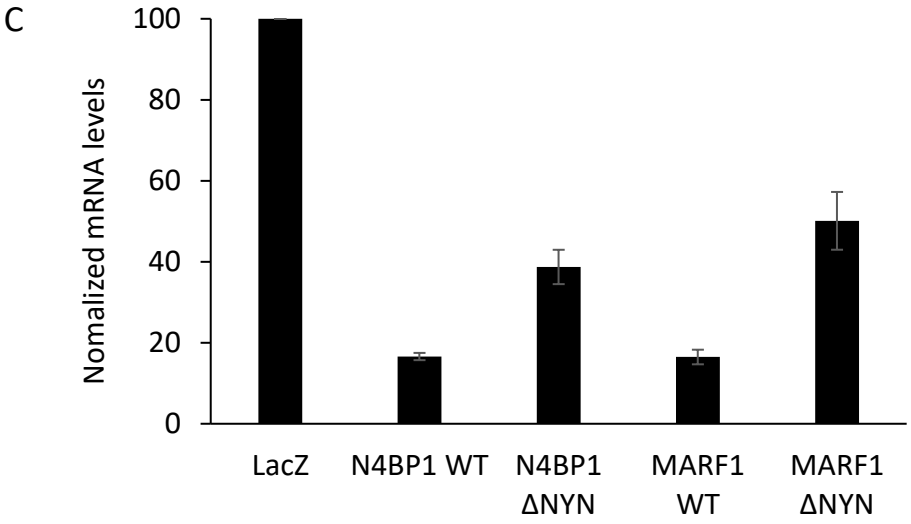
C
Nomalized mRNA levels
100
80
60
40
20
0
LacZ
N4BP1 WT
N4BP1 ΔNYN
MARF1 WT
MARF1 ΔNYN

Figure 8: **N4BP1 represses a tethered mRNA reporter to a similar extent the MARF1 endonuclease.** (A) Schematic representation of λNHA-MARF1, including nuclease (NYN), RNA binding domains (RRM1/2, LOTUS) and EDC4 binding (C-terminal) domain (as described in Brothers et al., 2020). (B) RL activity detected in lysates from 293T cells expressing the indicated protein, measured using a luminometer. Cells were co-transfected with plasmids expressing RL-5BoxB reporter, FL, and indicated tethered proteins. The chart represents normalized mean values of RL luminescence from 3 experiments. RL activity while tethered to λNHA-LacZ was set as 100. (C) RL mRNA levels detected in lysates of 293T cells expressing the indicated proteins., measured using RT-qPCR. Cells were co-transfected with plasmids expressing RL-5BoxB reporter, FL, and indicated tethered proteins as above. The chart represents the mean value of RL mRNA from 3 experiments. RL mRNA level while tethered to λNHA-LacZ was set as 100. Error bars represent SEM from multiple independent experiments. P-values were calculated using an unpaired two-tailed Student's T-test. *$p < 0.05$.

3.2 N4BP1 localizes primarily to the cytoplasm in human cells, and co-localizes with P-body proteins

Current understanding of N4BP1 illustrates that it functions both in the cytosol (regulating immune function; Gitlin et al., 2020) and nucleus (mediating post-translational modification; Sharma et al., 2010). To determine where WT-N4BP1 localizes in human cells, cell fractionation was performed on U-2 OS and HeLa cell lines. Cells were transiently transfected with FLAG-tagged full-length N4BP1, lysed 24 hours later in a hypotonic lysis buffer, and centrifuged to separate cytosolic and nuclear fractions. Whole cell, cytosolic and nuclear fractions of U-2 OS and HeLa cells were then analyzed using SDS-PAGE (sodium dodecyl sulfate-polyacrylamide gel electrophoresis) and western blotting (Figure 9). To determine whether the nuclear and cytosolic fractions were separated efficiently, GAPDH (cytosolic marker) and hnRNP (isoform A1, nuclear marker) levels were also evaluated in each fraction. In both cell lines N4BP1 appeared predominantly cytosolic; however, HeLa cells showed some expression in the nuclear fraction. A caspase-8 cleavage product of N4BP1 (identified in Gitlin et al., 2020), was found

only in the cytoplasm in both cell lines. While there was some hnRNPA1 found in the cytosolic fractions, GAPDH was found only in the cytosolic fraction and not in the nuclear fraction.

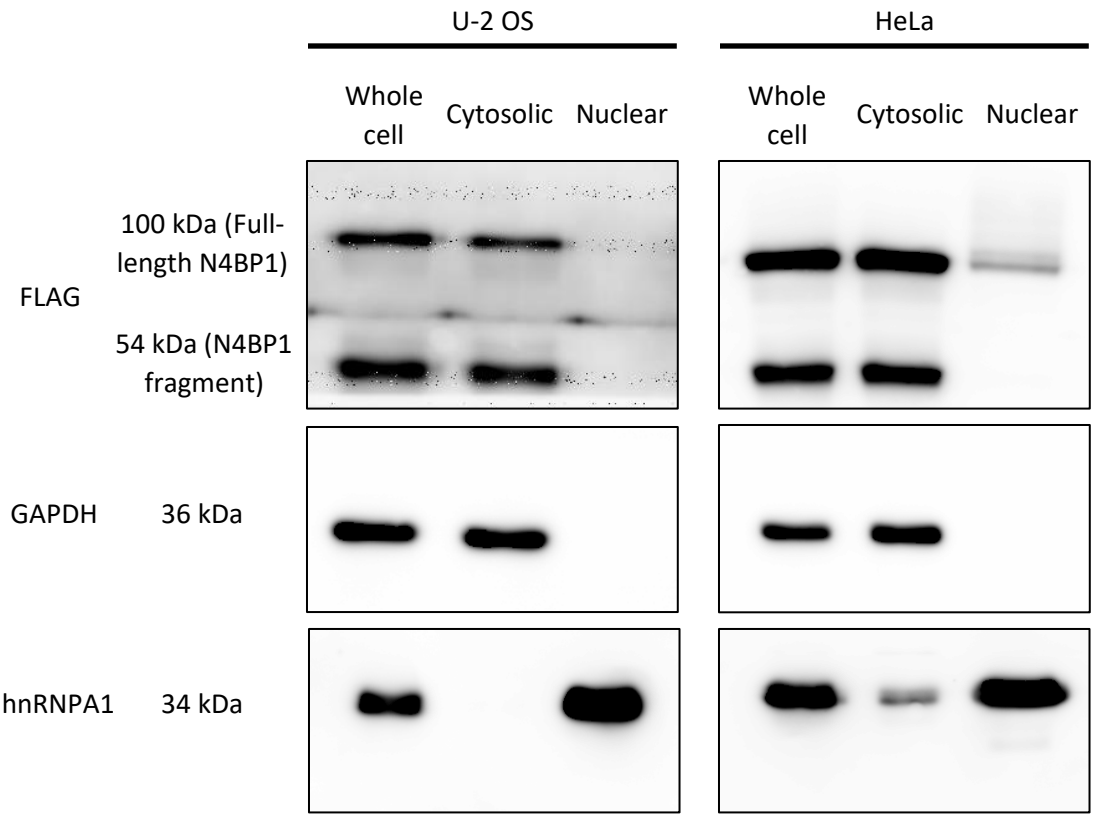

Figure 9: **N4BP1 localizes primarily to the cytosol in U-2 OS and HeLa cells.** Western blot of whole cell, cytosolic, and nuclear cell fractions of U-2 OS (left) and HeLa (right) cells following transfection with plasmids encoding FLAG-tagged WT-N4BP1. GAPDH (cytosolic) and hnRNPA1 (nuclear) were used as loading controls for their respective cellular fractions. A cleavage product of N4BP1 identified by Gitlin et al. (2020), was also identified in this experiment and is depicted below full-length N4BP1.

FLAG-tagged N4BP1 localization was next analyzed in live cells using immunofluorescence and confocal microscopy. HeLa cells were transiently transfected with desired constructs, fixed 24 hours later to a glass slide using paraformaldehyde, permeabilized using a detergent, and blocked using a 4% BSA solution. Cells were then probed with primary antibodies, washed, then incubated with fluorescent secondary antibodies, and mounted on a microscope slide prior to analysis via confocal microscopy. FLAG-tagged N4BP1 localized to the cytosol in most cells, and localized to numerous discrete foci (Figure 10A, left panel) that were reminiscent of P-bodies. A recent Bio-ID screen investigating protein-protein associations in mammalian cells identified N4BP1 in proximity to several proteins that also localize to P-bodies, including the miRNA-associated protein GW182, and the mRNA decapping factor DCP1 (Youn et al., 2018). To assess whether N4BP1 was indeed localizing to P-bodies, I carried out immunofluorescent analysis using an antibody for a P-body marker, EDC4 (Figure 10A, middle panel). We observed strong colocalization of FLAG-tagged N4BP1 and endogenous N4BP1 in HeLa cells (Figure 10A). This colocalization was also assessed by co-transfecting plasmids encoding FLAG-tagged N4BP1 and V5-tagged EDC4 (Figure 10B). Both endogenous (Figure 10A) and ectopically expressed (Figure 10B) EDC4 co-localize with N4BP1 in the cytoplasm of HeLa cells. Importantly, while there was some clear localization of N4BP1 to the nucleus in cells with endogenous levels of EDC4 expression (Figure 10A), cells overexpressing EDC4 had no visible nuclear N4BP1. Further, in cells without ectopic expression of EDC4 or N4BP1, EDC4 was diffusely distributed throughout the cytoplasm; N4BP1 overexpression induced formation of foci with EDC4 resembling P-bodies in the cytoplasm. Similar trends were noticed with N4BP1 and another marker of P-bodies, DCP1 (Figure 10C). In this figure, N4BP1 could not only localize to

the nucleus but also form nuclear foci, while DCP1 localized solely to the cytoplasm. Taken together, these data indicate that N4BP1 can localize in P-bodies in HeLa cells.

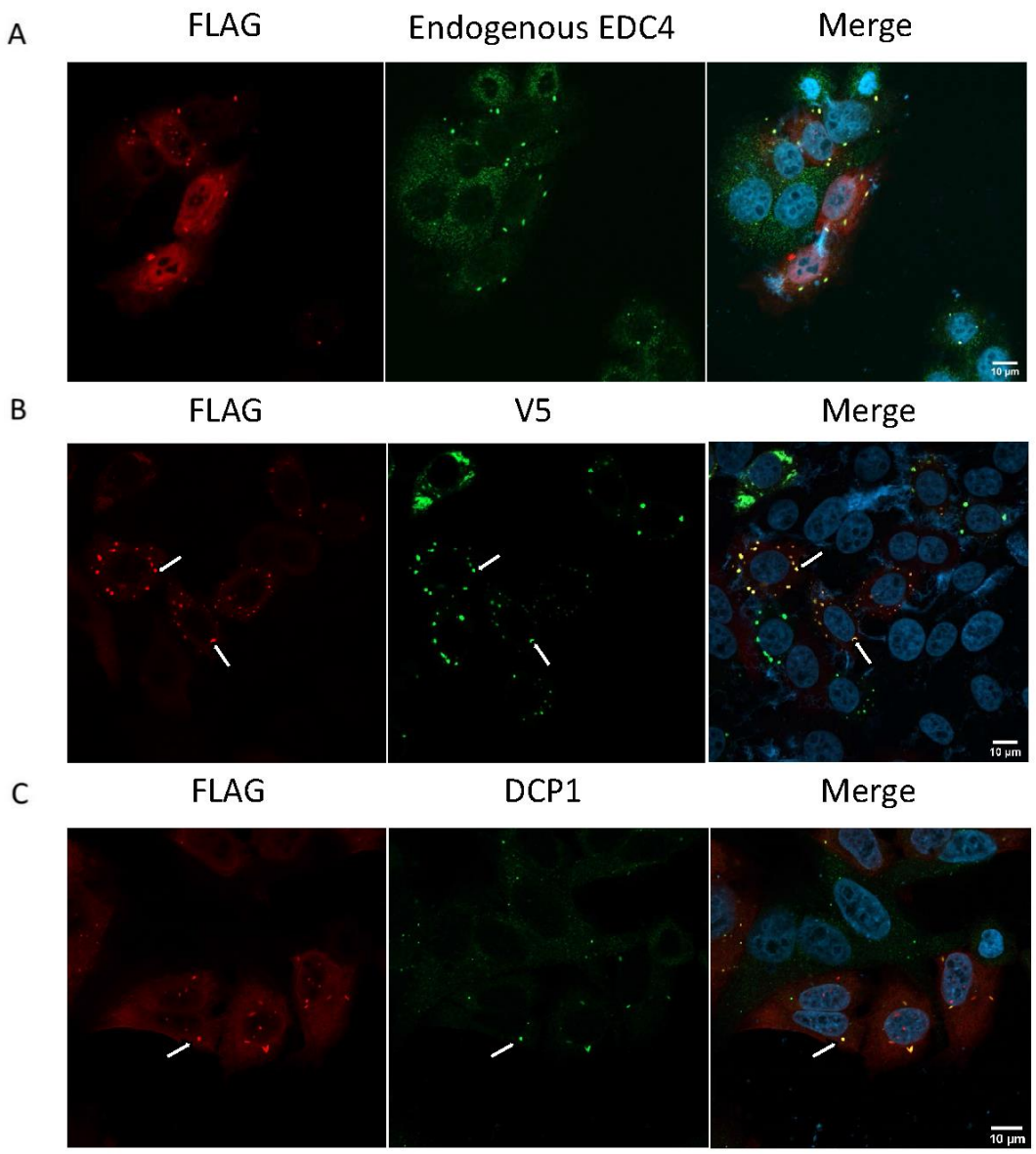

Figure 10: **N4BP1 localizes to both the cytoplasm and nucleus, and co-localizes with P-body markers in the cytosol of HeLa cells.** Confocal fluorescence micrograph of HeLa cells transfected expressing FLAG-tagged WT N4BP1, as well as P-body proteins (green) including endogenous EDC4 (A), ectopic V5-tagged EDC4 (B), and endogenous DCP1 (C). DAPI was used to stain nucleic acids (blue). White arrows mark sites of co-localization. Representative fields were selected from three biological replicates.

3.3 The central region of N4BP1 dictates its nuclear localization while its N-terminal region is responsible for P-body localization

Since N4BP1 can be found in both the cytoplasm and nucleus, it is still left to question what dictates differential N4BP1 localization. To address this question, plasmids were generated expressing N4BP1 fragments containing the N-terminal domain including the KH domain (Fragment 1, residues 2-296), a linker region (Fragment 2, residues 268-601), and a C-terminal domain containing the NYN and CoCUN (ubiquitin binding) domains (Fragment 3, residues 575-896) (see Figure 6). HeLa cells were transfected with these constructs along with a plasmid coding for V5-tagged EDC4, and immunofluorescent analysis was carried out as previously described (Figure 11). Fragments 1 and 3 localized to the cytoplasm, however, only fragment 1, which contains the N-terminal KH domain, co-localized with V5-tagged EDC4 in P-bodies. In contrast, a fragment of N4BP1 that contains the linker region (Fragment 2) displayed a strong nuclear localization.

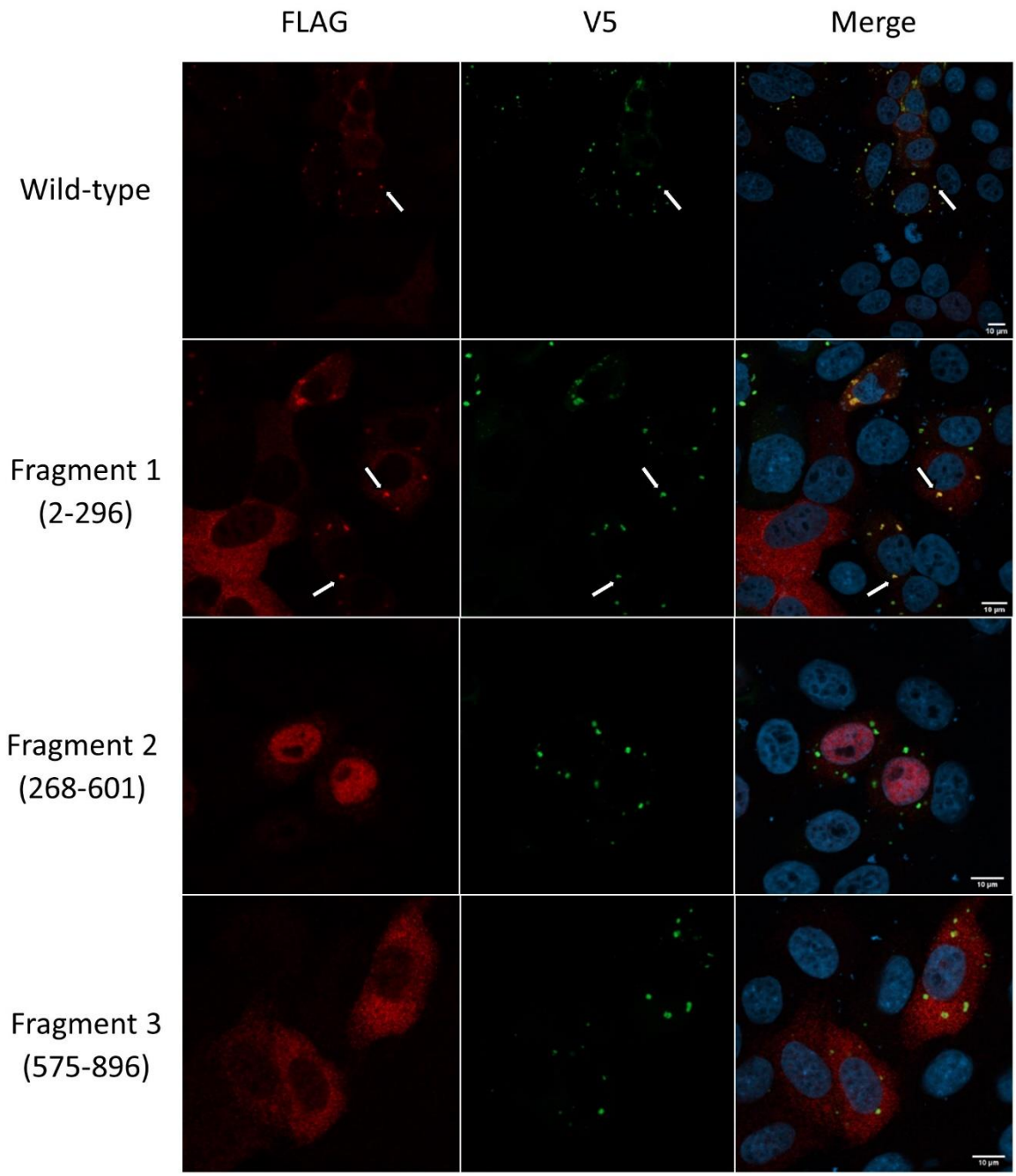

Figure 11: **N4BP1 fragments are differentially localized in HeLa cells.** Confocal fluorescence micrograph of HeLa cells transfected expressing FLAG-tagged (red) N4BP1 WT, Fragment 1 (N-terminal, KH domain, residues 2- 296), Fragment 2 (linker, residues 268-601), and Fragment 3 (C-terminal, NYN and CoCUN domains, residues 575-896), as well as overexpressed V5-tagged EDC4 (green). DAPI was used to stain nucleic acids (blue). White arrows mark sites of co-localization. Representative fields were selected from three biological replicates.

To assess whether N4BP1 localization is cell-type specific, immunofluorescent confocal microscopy was performed on U-2 OS cells expressing FLAG-tagged N4BP1 and V5-tagged EDC4 (Figure 12). Similar trends were found between HeLa and U-2 OS cells, with WT N4BP1 localizing to either the nucleus or cytoplasm (A), the N-terminal fragment containing the KH domain localizing to the cytoplasm and co-localizing with EDC4 (B) and the linker fragment localizing to the nucleus (C). These data therefore suggest that the N-terminal region (containing the KH domain) is responsible for co-localization of N4BP1 with EDC4, while the internal linker region of N4BP1 is responsible for localizing N4BP1 to the nucleus.

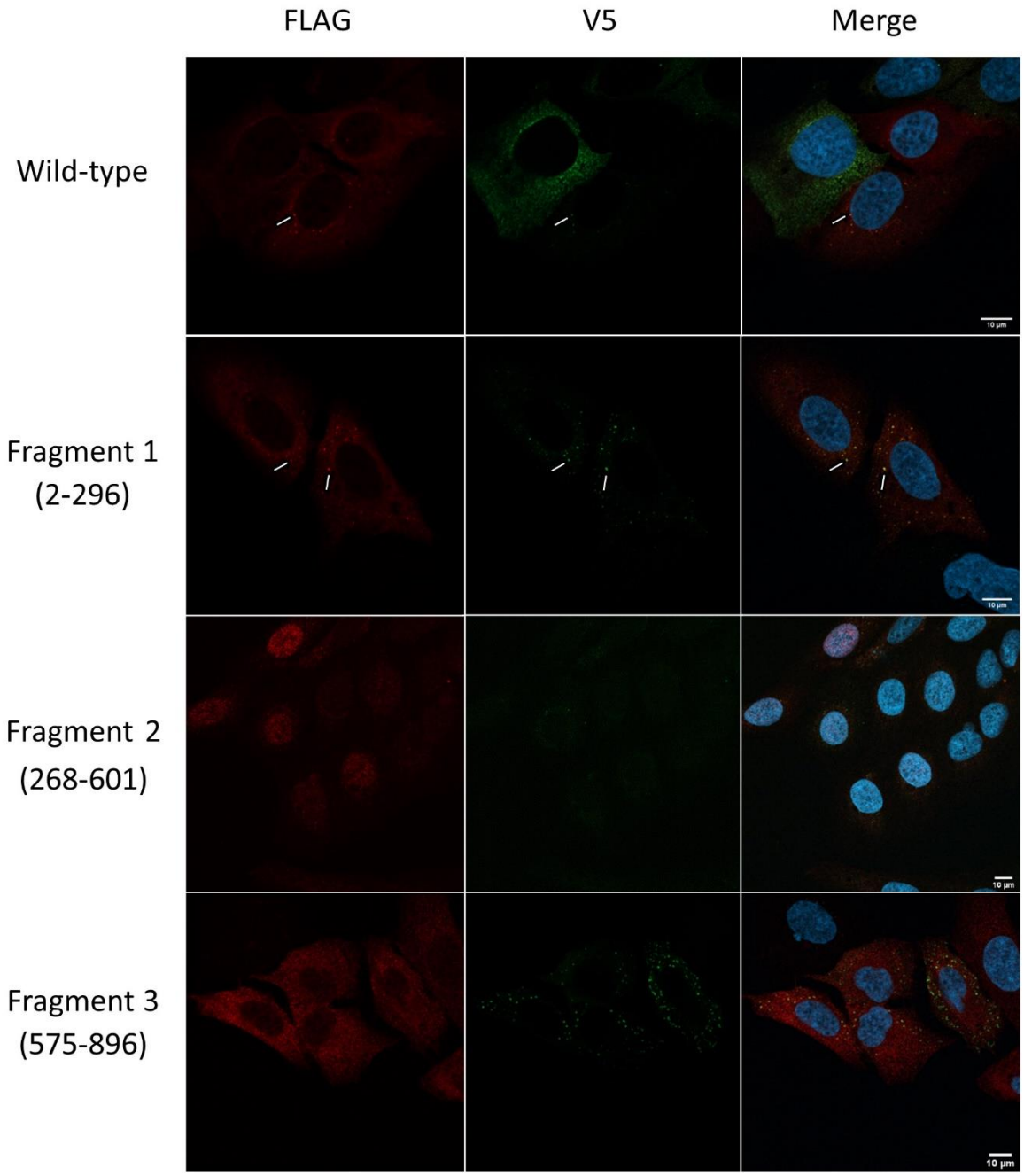

Figure 12: **N4BP1 fragments are differentially localized in U-2 OS cells.** Confocal fluorescence micrograph of U-2 OS cells transfected expressing FLAG-tagged (red) N4BP1 WT, Fragment 1 (N-terminal, KH domain, residues 2- 296), Fragment 2 (linker, residues 268-601), and Fragment 3 (C-terminal, NYN and CoCUN domains, residues 575-896), as well as overexpressed V5-tagged EDC4 (green). DAPI was used to stain nucleic acids (blue). White arrows mark sites of co-localization. Representative fields were selected from three biological replicates.

3.4 Towards identifying N4BP1-interacting proteins in human cells

To further assess how N4BP1 localizes to the nucleus or cytoplasm and determine the roles of N4BP1 in different cell compartments, this project next aimed to identify N4BP1-interacting proteins. To do so U-2 OS cells stably expressing V5-tagged N4BP1were generated, lysed, and immunoprecipitated using a V5 antibody as described above. Rather than western blotting, immunoprecipitated samples were sent in biological triplicate for mass spectrometry analysis at the Lady Davis Institute proteomics core (Montreal, QC). Control V5-immunoprecipitations were also performed on non-transduced U-2 OS cells to identify background peptides in our samples. Table 1 (Appendix A) and Figure 13 illustrate N4BP1 interacting proteins, selected based on having: a p-value < 0.05, at least a 2-fold increase in abundance in N4BP1 stably expressing cells compared to control, and non-significant enrichment in the Contaminant repository for affinity purification (CRAPome; < 20/411). The CRAPome is a repository for proteins that are non-specifically pulled down in affinity mass-spectrometry experiments, acting as a negative control (Mellacheruvu et al., 2013). As expected, interacting proteins were found that localized to the cytosol (KIAA1522; Liu et al. 2016), and nucleus (Coronin 2a; Huang et al. 2011). The most highly enriched protein identified was KIAA1522, which is a yet uncharacterized protein shown to act as an oncogene in the KRAS pathway (Liu et al. 2016). Intriguingly, numerous proteins that were identified on this list are involved in actin dynamics, including coronins 2a and 2b, MISP and PALM (Huang et al. 2011, Schwarz et al. 2019, Zhu et al. 2013, Turk et al. 2012); this suggests that N4BP1 may be involved in regulating actin dynamics itself, or that actin dynamics could dictate its function/localization. Further, coronin 2a, RAPH1 and CD58 (Sun et al. 2021, Gollob and Ritz, 1996) are proteins involved in the immune

response (via modulating actin dynamics, T-cell trafficking, and T-cell receptor-ligand interactions), supporting the notion in the literature that N4BP1 plays a role in the immune response. Coronins 2a and 2b have 61% identity with each other, giving strong evidence that coronins interact with N4BP1. An E3-ubiquitin ligase RFWD3 was also identified, illustrating that N4BP1 may play a role in protein ubiquitylation in U-2 OS cells. Of note, flotillin-1 is a protein involved in the endocytic pathway, and SUMOylation of this protein leads to its nuclear localization (Jang et al. 2019). Since SUMOylation dictates N4BP1 localization between the nucleolus and PML bodies in mouse embryonic fibroblasts (Sharma et al. 2010), the interactions with flotillin-1 may shed light on the mechanism of N4BP1 nuclear localization. As well, EDC4 was identified in this analysis to be enriched 2-fold in the stably expressing cells compared to control, just barely missing the significance cut-off at $p = 0.079$.

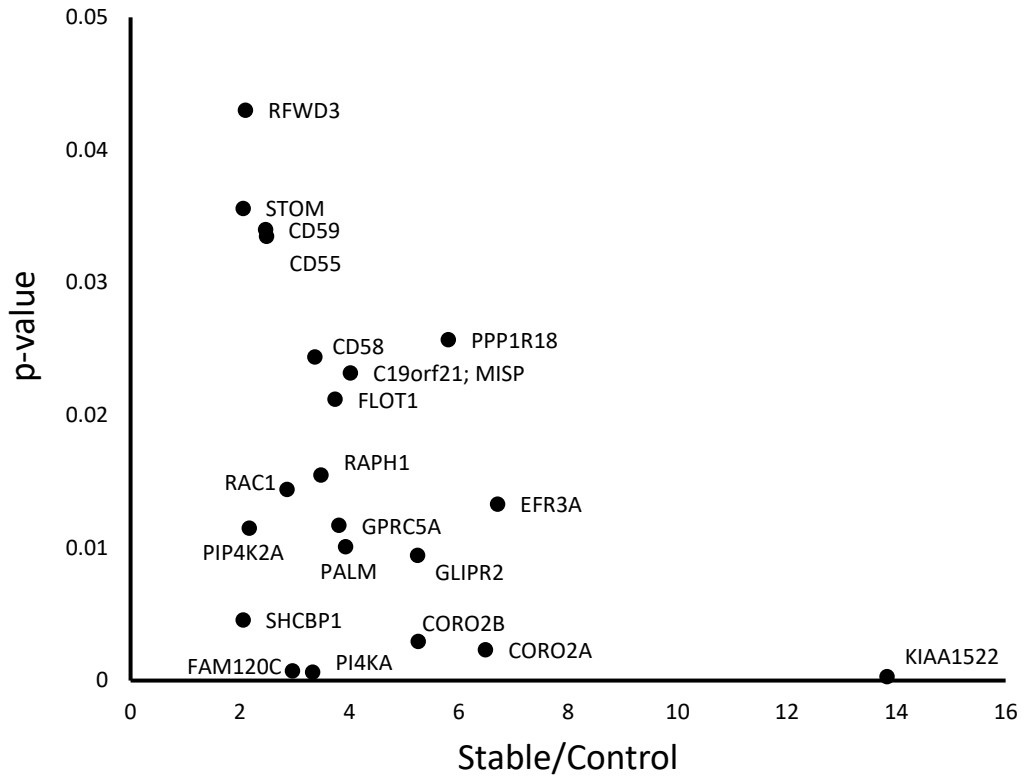

Figure 13: **N4BP1 interacts predominantly with nuclear proteins in U-2 OS cells**. Proteins identified from mass spectrometry following immunoprecipitation of stably expressing V5-tagged N4BP1 in U-2 OS cells. Proteins were selected based on having: a ratio of ≥ 2.00 for the abundance co-immunoprecipitated from N4BP1 stably expressing cells compared to control cells (Stable/Control); p-value > 0.05; insignificant (≤ 20/411) abundance of protein in CRAPome database. The x-axis represents fold enrichment of proteins isolated from N4BP1 stably expressing cells compared to control cells. The y-axis illustrates the p-value for the difference in protein isolated between N4BP1 stably expressing and control groups.

Lastly, to assess the function of N4BP1 and its variability across different cell lines, HeLa cells stably expressing V5-N4BP1 were generated to perform immunoprecipitation and mass spectrometry as discussed above. In hopes of improving N4BP1 expression and yield from immunoprecipitation, a pLEX vector was used for stable expression rather than pLENTI6, and a different lysis buffer was used than in the U-2 OS experiment (see methods).

When compared to data acquired using U-2 OS cells (Tables 1 & 2), the bait protein N4BP1 was further enriched in the HeLa cell experiment (~100 fold compared to 56.98 in U-2 OS), had better protein coverage (63% compared to 51%) and more protein unique peptides identified (68 compared to 39). Similar trends were found across identified protein interactors as well, suggesting that N4BP1 and interacting proteins were more efficiently isolated in the HeLa experiment than in the U-2 OS experiment. As a result of higher data quality, candidate interacting proteins for N4BP1 were assessed differently in the HeLa experiment. Proteins were selected based on: enrichment of at least 5-fold in the stably expressing cells compared to control cells; $p<0.05$; average number of spectral counts in the CRAPome < 10; and number of protein unique peptides identified ≥ 2.

Proteins were identified that localize to the nucleus (LEMD3), nucleolus (SPTY2D1), secretory pathway (DAB2) and mitochondria (CYCS) (Figure 14, Hellemans et al., 2004, Chambers et al., 2018, Osakabe et al., 2013, Figliuolo et al., 2020, Ow et al., 2008). Importantly, there were numerous proteins identified to be involved in protein modification, including E-3 ubiquitin ligase activity (DDB1 and KCTD10), and proteins isomerase PDIA4, supporting the notion that N4BP1 interacts with PML body proteins and is involved in facilitating protein modifications (Fischer et al., 2014, Nagai et al., 2018, Wang et al., 2020).

N4BP1 was also identified to interact with various proteins involved in regulating the NF-κB pathway including MTDH and DAB2. Intriguingly, DAB2 regulates NF-κB activity via TRIF dependent TLR signalling (Shi & Wang, 2015, Figliuolo et al., 2020). Further, proteins were identified that are involved in other aspects of the immune system including dermcidin, involved in innate immunity via antimicrobial activity in secretions, and DBNL, involved in T-cell activation (Schittek, 2012, Rocha-Perugini et al., 2017).

Interactions of N4BP1 with endoplasmic reticulum, Golgi, endocytic and mitochondrial proteins may be explained in several ways. Firstly, the identified proteins could be true interactors, illustrating novel roles of N4BP1 in these cellular compartments. On the other hand, since N4BP1 was highly expressed and efficiently immunoprecipitated, it is possible that some N4BP1 was isolated while being translated or travelling through the secretory system on route to its destination. However, the interactions of N4BP1 with endosomal and mitochondrial proteins cannot be easily explained by this hypothesis. A final possibility is that N4BP1 could be mediating turnover of these proteins via previously characterized roles in ubiquitylation and proteasomal degradation.

There were several proteins that narrowly missed the cutoff criteria but still are worth noting. EDC4 just missed the significance cutoff ($p = 0.06$), while still being strongly enriched in the stably expressing group and having multiple protein specific peptides identified. What is more, LSM12, a protein that can localize to P-bodies was excluded due to the identification of solely 1 protein specific peptide (Swisher & Parker, 2010). Other proteins that were narrowly excluded similarly to EDC4 and LSM12 are as follows: PABPC4 (mRNA regulation), PAIP1 (mRNA regulation via PABP), RANBP2 (Protein SUMO-ligase), ZNRF2 (E3 ubiquitin-ligase), and PSMA1 (proteasome subunit) (Kini et al., 2014, Lv et al., 2014, Moreno-Oñate et al., 2020,

Araki & Milbrandt, 2003, Ding et al., 2020). While these proteins were excluded from Figure 14 and Table 2, it is still possible that they interact with N4BP1 and offer some insight into the role of N4BP1 in mRNA regulation and protein modifications.

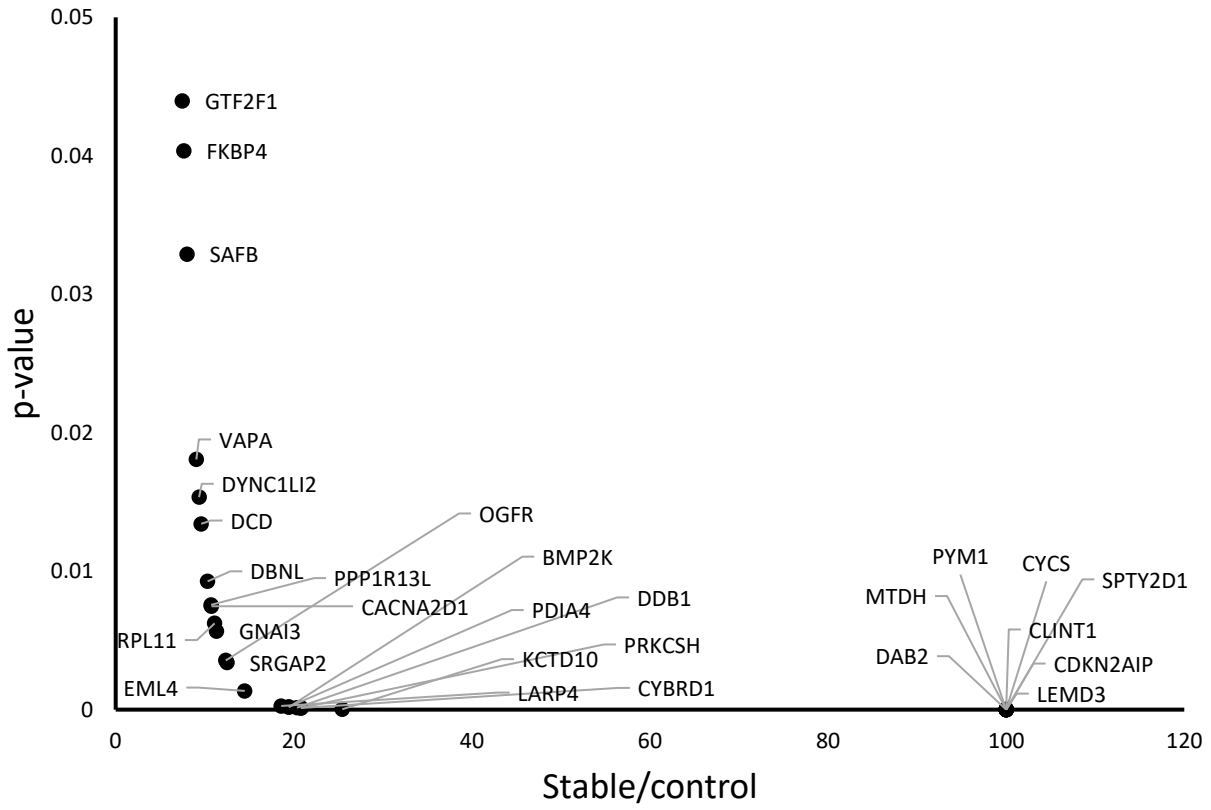

Figure 14: **N4BP1 interacts with proteins found in the nucleus, nucleolus, secretory system and mitochondria in HeLa cells**. Proteins identified from mass spectrometry following immunoprecipitation of stably expressing V5-tagged N4BP1 in HeLa cells. Proteins were selected based on having: a ratio of ≥ 5.00 for the abundance co-immunoprecipitated from N4BP1 stably expressing cells compared to control cells (Stable/Control); p-value > 0.05; < 10 spectral counts on average in the CRAPome database, and ≥ 2 protein unique peptides identified. The x-axis represents fold enrichment of proteins isolated from N4BP1 stably expressing cells compared to control cells. The y-axis illustrates the p-value for the difference in protein isolated between N4BP1 stably expressing and control groups.

3.5 N4BP1 does not display clear interactions with EDC4 in HeLa cells

Since ectopic EDC4 co-localized with N4BP1 in HeLa and U-2 OS cells, and barely missed the mass spectrometry cut off for significance, it was next assessed whether there was a direct interaction between these proteins in HeLa cells. To test this possibility, co-immunoprecipitation was performed on cells transiently transfected with FLAG-tagged N4BP1 and V5-tagged EDC4 using a FLAG antibody. MARF1 is a NYN encoding nuclease that has been shown to interact with EDC4 via its C-terminal domain, and this interaction motif was used as a positive control (Nishimura et al., 2018). Transfected cells were lysed using a hypotonic buffer, pre-cleared of non-specific binding proteins by incubation of lysates with protein-G agarose beads, then immunoprecipitated using FLAG-M2/protein-G agarose beads, and then visualized using SDS-PAGE and western blotting. Inputs represent 3% of the total lysate, taken prior to immunoprecipitation. Figure 15 illustrates that while EDC4 was found clearly in the immunoprecipitated fraction in MARF1 transfected cells, it was minimally detected in the immunoprecipitation fraction of N4BP1 transfected cells. These data suggest that N4BP1 does not directly interact with EDC4.

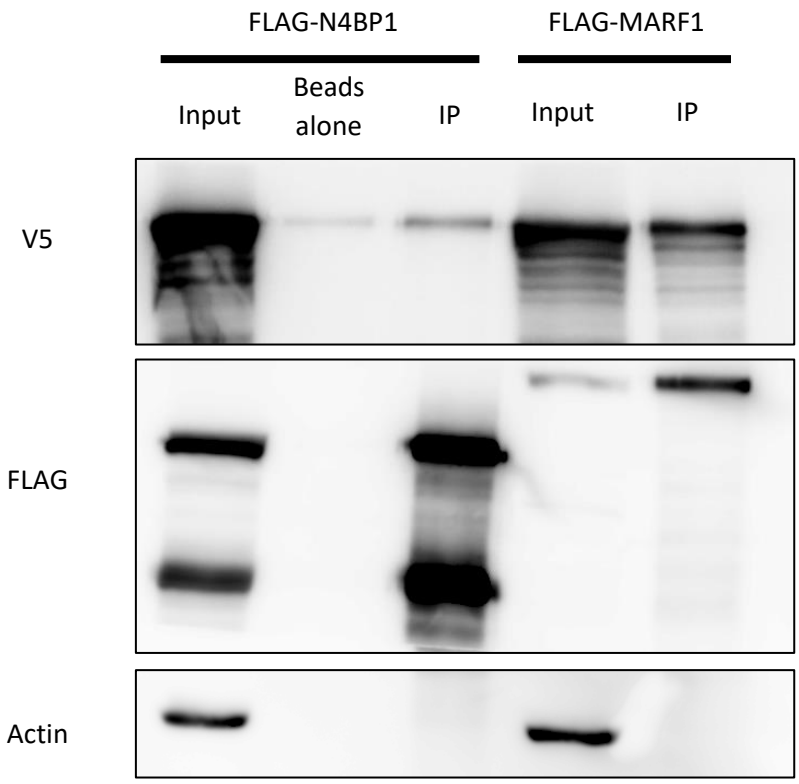

Figure 15: **N4BP1 does not physically interact with EDC4 in HeLa cells**. Co-immunoprecipitation of FLAG-tagged N4BP1 and MARF1, and western blotting for FLAG proteins and associated ectopic V5-tagged EDC4 (N=3). β-Actin was used as a loading control. Proteins were immunoprecipitated using mouse-FLAG-M2 antibodies on protein G agarose beads. Inputs represent addition of lysate (3% of total), taken prior to immunoprecipitation. IP = immunoprecipitation.

Discussion

N4BP1 represses the expression of a tethered mRNA dependent on its NYN domain

This project set out to investigate whether N4BP1 is capable of post-transcriptionally repressing gene expression. To this end, I used several different approaches to investigate N4BP1-mediated gene silencing, N4BP1 localization and to identify proteins that may interact with N4BP1 in mammalian cells.

My data indicate that N4BP1 can repress the expression of a reporter mRNA when artificially tethered to it using a dual-luciferase reporter system (Figures 7 and 8), suggesting that direct RNA binding by N4BP1 is not required for it silencing a mRNA. N4BP1 not only reduced the protein expression of a tethered reporter, as measured by luminescence (Figure 7B), but also decreased the abundance of that mRNA, as measured by RT-qPCR (Figure 7C). Importantly, this repression was dependent on the activity of the NYN domain of N4BP1. A D623N point mutant, previously described to ablate NYN-mediated viral RNA repression (Yamasoba et al., 2019) caused slight de-repression of N4BP1-mediated silencing of protein activity. On the other hand, deleting the entire NYN domain led to significantly less repression (Figure 7B). Further, the D623N mutation did not cause a de-repression of N4BP1 mediated mRNA decay (Figure 7C), while the ΔNYN mutation did. Lastly, tethering N4BP1 to a reporter mRNA repressed it to a similar degree as compared to MARF1, a NYN-containing protein with established endonuclease activity (Figure 8). Taken together, these data are consistent with the hypothesis that N4BP1 can dictate the decay of a targeted mRNA in human cells, and this is done in a manner that is dependent on its NYN domain.

The fact that a D623N mutation did not ablate N4BP1 mediated mRNA decay was surprising – Yamasoba et al. (2019) used the D623N point mutation as a model for relieving

N4BP1-mediated HIV repression. In this paper it was shown that the D623N mutation not only ablated the N4BP1 mediated immune response to HIV, but also that only D623N (and not WT) N4BP1 co-immunoprecipitated HIV RNAs. Furthermore, making the analogous point mutation in KHNYN (the N4BP1 paralog) prevented the ability of KHNYN to repress HIV RNAs (Nepravishta et al., 2019). However, the findings in this thesis do not altogether contradict the literature. Both Yamasoba et al. (2019) and Ficarelli et al. (2019) did not utilize a tethered mRNA system. It is possible that when a mRNA is bound by N4BP1 (as when tethered), the other aspartic acid residues in the catalytic core of the NYN domain of N4BP1 could compensate for the mutation and still induce transcript cleavage. It is likely that endogenous or viral mRNAs targeted by N4BP1 (e.g. HIV mRNA) would be in contact with N4BP1 for a shorter time, and thus a D623N mutation may be sufficient to cause de-repression. Lastly, it is also possible that N4BP1 interacts with mRNA decay proteins dependent on its NYN domain, and thus removing the NYN domain would disrupt these interactions and cause de-repression, while the D623N point mutation may not.

While N4BP1 induces the decay of a tethered transcript, it is not yet clear whether this is directly due to the nuclease activity of N4BP1, or due to interactions with other mRNA decay proteins (e.g. EDC4). For example, Roquin-1 can target mRNAs involved in the immune response using its RNA binding domains, but coordinated proteins in the de-adenylation-dependent mRNA decay pathway (e.g. CCR4-NOT) to degrade transcripts (Mino & Takeuchi, 2015). In support of this notion, Gitlin et al. (2020) found that N4BP1 repressed many mRNAs involved in the immune response by RNA-sequencing, but it was later shown that N4BP1 regulates transcription factor NF-κB at the protein level, accounting for this mRNA repression (Shu et al., 2021). Thus, while the findings above offer strong supporting evidence that N4BP1

can act as a nuclease to degrade mRNAs, further experimentation must be done to determine whether this decay is a direct consequence of N4BP1 nuclease activity, or via interactions with N4BP1-binding proteins.

N4BP1 can localize either to the cytosol or nucleus in HeLa and U-2 OS cells

N4BP1 has been shown to have distinct roles in either the cytoplasm (human macrophages) or nucleus (mouse embryonic fibroblasts) (Gitlin et al., 2020, Sharma et al., 2010). However, it is unclear what dictates N4BP1 localization between these compartments, and how this localization varies between cell types. To assess these questions, cell fractionation and immunofluorescent analysis were carried out on HeLa and U-2 OS transiently transfected with FLAG-tagged N4BP1. In cell fractionation experiments, N4BP1 was found predominantly in the cytosol, but not in the nucleus of either HeLa or U-2 OS cells (Figure 9). However, there was some N4BP1 found in very low abundance in the nuclear fraction of HeLa cells. Further, using immunofluorescent analysis (Figure 10), N4BP1 was found predominantly in the cytosol of HeLa cells. These findings strongly support the notion that N4BP1 has a primarily cytosolic role in mammalian cells, supporting limited literature data in human macrophages (Gitlin et al., 2020).

N4BP1 was identified in proximity to the decapping protein DCP1 (Youn et al., 2018), which localizes to P-bodies. This project therefore sought to assess whether DCP1 and other P-body proteins co-localized in human cell lines. In HeLa cells, FLAG-tagged N4BP1 clearly co-localized with both endogenous (A) and ectopically expressed (B) EDC4 in cytosolic foci (Figures 10A and B) and with endogenous DCP1 (Figure 10C). Thus, N4BP1 has the capacity to localize to P-bodies in mammalian cells. Intriguingly, while N4BP1 appeared predominantly cytosolic in HeLa cells, there was still some nuclear staining either diffusely or in foci.

Therefore, N4BP1 localizes both to the nucleus and cytosol, supporting literature findings in human macrophages and MEF (mouse embryonic fibroblast) cells (Gitlin et al., 2020, Sharma et al., 2010). As such, while the primary localization of N4BP1 may vary between cell types or by species (being predominantly nuclear in MEFs, but cytoplasmic in human macrophages), the findings above suggest that N4BP1 can act in both sites within one cell-type. Nonetheless, identification of a yet uncharacterized role of N4BP1 in P-bodies expands on the already diverse function of this protein.

To determine what dictates differential N4BP1 localization to the nucleus and cytoplasm, fragments of N4BP1 were cloned into a FLAG-tagged vector (Figure 6) and were assessed using immunofluorescent analysis. The fragments were generated as follows: a N-terminal domain including the KH domain (residues 2-296), a linker domain containing MALT1 and Caspase-8 cleavage sites (residues 268-601), and a C-terminal domain containing the NYN and CoCUN (ubiquitin binding) domains (residues 575-896) (see Figure 6). When these fragments were ectopically expressed in HeLa cells, the central linker fragment was found to be predominantly nuclear, while both the N-terminal (KH domain) and C-terminal (NYN, CoCUN domains) fragments were cytosolic (Figure 11). Further, co-expression of V5-EDC4 illustrates that only the N-terminal (KH domain) fragment was able to colocalize with EDC4 in cytosolic foci. Since the KH domain of N4BP1 has the potential to bind RNA, it is not altogether clear whether N4BP1 (WT and the N-terminal fragment) localizes to P-bodies via interactions with RNA or proteins. Nonetheless, these results illustrate that the N-terminal region dictates localization to cytosolic foci. What is more, since only the central linker region was found predominantly in the nucleus, it is likely that this fragment dictates the nuclear localization of N4BP1. While there is no clear nuclear or nucleolar localization sequence found in this region, there is a predicted

ubiquitin binding domain there (Gitlin et al., 2020). It has already been shown that SUMOylation dictates the localization of N4BP1 between the nucleolus and PML bodies in the nucleus of MEF cells (Sharma et al., 2010), so it is not unreasonable to speculate that other post translational modifications could dictate N4BP1 localization between the cytosol and the nucleus. While further characterization of N4BP1 domains is necessary, these experiments offer insight into how N4BP1 may exert its functions in cells.

Since there is significant variation among N4BP1 localization between cell lines in the literature, I assessed whether the localization of N4BP1 differed between HeLa and U-2 OS cell lines. Similar trends were found in U-2 OS cells, where WT and both the N-terminal (KH domain) and C-terminal (NYN, CoCUN domains) fragments were found mostly in the cytosol, and the linker fragment was found in the nucleus (Figure 12). Further, only WT and the N-terminal fragment co-localized with ectopically expressed EDC4 in cytosolic foci. Notably, although P-bodies look markedly different between HeLa and U-2 OS cell lines, trends of N4BP1 and EDC4 localization remained the same.

Altogether, these results lend significant insight to the current literature understanding of the role of N4BP1. While studies have shown that N4BP1 can have specifically nuclear or cytoplasmic roles in different cell lines, the findings above make clear that N4BP1 can be found in both sites simultaneously in human cells. Most importantly from this research, N4BP1 has a yet entirely uncharacterized role in the cytoplasm through its interactions with P-body proteins. Furthermore, by identifying the regions of N4BP1 which dictate localization to the nucleus (central linker fragment) and P-bodies (N-terminal, KH domain containing fragment), these findings lay a foundation for further studies to assess how N4BP1 translocates between regions of the cell.

N4BP1-protein interactome

All previous studies assessing N4BP1-protein interactions made use of protein specific co-immunoprecipitation experiments (Oberst et al., 2007, Spel et al., 2018, Gitlin et al., 2020, Shi et al., 2021), but large-scale proteomic analysis of N4BP1 interactions is absent from the literature. Such large-scale experiments would provide critical insight into how N4BP1 exerts its diverse functions. To identify N4BP1 protein interactors, stably expressing V5-N4BP1 was immunoprecipitated in U-2 OS cells, followed by affinity mass spectrometry. The proteins that were identified to be significantly enriched ($p < 0.05$, $\geq$ 2-fold increase in N4BP1 stably expressing cells compared to control), and not found commonly in the CRAPome, are illustrated in Figure 13 and Table 1. Of concern, the bait protein N4BP1 had less enrichment than expected (56.98 compared to 100, which would indicate that it was found only in the stably expressing cells). While this is still significant enrichment, inefficient pull-down of N4BP1 could severely impact isolation of interacting proteins. Nonetheless, proteins identified in this screen localized to the cytosol (e.g. KIAA1522), and nucleus (e.g. Cononin 2a). Of the proteins found, functional themes were identified including control of actin dynamics (coronin2a and 2b, MISP and PALM), immune regulation (Coronin 2a, RAPH1 and CD58), and protein modification (RFWD3). These themes support the notion in the literature that N4BP1 regulates immune functions in mammalian cells, and that it plays a role in regulating ubiquitylation (Gitlin et al., 2020, Sharma et al., 2010). However, N4BP1 has been shown to regulate immune response via repression of viral RNAs and ubiquitylation of NF-κB (Shi et al., 2021); proteins involved in these pathways were not identified in the proteomic screen. It is possible that Coronin 2a, RAPH1 and PALM represent novel pathways through which N4BP1 regulates the immune response by modulating actin dynamics, or T-cell trafficking and activation. Intriguingly, while

N4BP1 has been shown to interact with E3 ubiquitin ligases (Nedd4 and ITCH) (Santonico, 2020, Oberst et al., 2007), the appearance of RFWD1 (another E3 ligase) in this screen suggests that N4BP1 may interact with a wider range of protein modifying enzymes depending on cell type, or could interact with these proteins non-specifically in sites such as PML bodies.

To assess whether protein interactions of N4BP1 differ between cell types, mass spectrometry analysis was performed in HeLa cells stably expressing V5-tagged N4BP1. To improve yield of co-immunoprecipitated N4BP1, a pLEX expression vector was used rather than pLENTI6, and the composition of lysis buffer was changed (see methods). As a result, the bait protein N4BP1 had a higher protein coverage (63% compared to 51%), protein unique peptides (68 compared to 39), fold enrichment (~100 fold compared to 56.98 in U-2 OS), and lower p-value (1.61E-16 compared to 8.95E-03) in the HeLa screen than in the U-2 OS screen. Due to the improved isolation of N4BP1, more stringent conditions were required to make a succinct list of interacting proteins, including: enrichment of at least 5-fold in the stably expressing compared to control cells, $p<0.05$, average number of spectral counts in the CRAPome < 10, and number of protein unique peptides identified ≥ 2 (Figure 14, Appendix A Table 2). Proteins were identified that reside in the nucleus (LEMD3), nucleolus (SPTY2D1), secretory pathway (DAB2) and mitochondria (CYCS). Further, several proteins were identified in the HeLa experiment that are involved in protein modifications within the nucleus, including E-3 ubiquitin ligase activity (DDB1 and KCTD10), and protein isomerase PDIA4. These interactions support the notion that N4BP1 interacts with protein modification enzymes in the nucleus. Also identified in this screen were multiple proteins involved in the NF-κB pathway of immune activation (MTDH and DAB2), and other components of the immune response including dermcidin (antimicrobial activity), and DBNL (T-cell activation). Thus, this data supports the idea that N4BP1 interacts

with protein modifying enzymes in the nucleus, and that N4BP1 regulates the immune response via interactions with the NF-κB pathway.

The purpose of performing affinity mass spectrometry for N4BP1 in both HeLa and U-2 OS cells was to determine whether N4BP1-protein interactions differ between cell types. There were no shared proteins identified across both screens. Further, while both experiments identified proteins involved in immune function, N4BP1 was found to interact with proteins in the NF-κB pathway only in HeLa cells. In addition, there were multiple protein modifying enzymes identified in the HeLa screen (DDB1 and KCTD10, and PDIA4), in contrast to only one protein modification enzyme in the U-2 OS screen (RFWD1). Thus, the results from HeLa cells, but not U-2 OS cells, strongly support literature findings that N4BP1 plays roles in immune regulation via the NF-κB pathway and interacts with protein modifying enzymes.

Agreement with literature, along with the improvement in bait protein N4BP1 isolation in the HeLa screen (unique peptides, protein coverage and p-value) suggest that while the HeLa screen identified real protein interactors of N4BP1, the U-2 OS screen may have yielded inaccurate findings. Indeed, higher expression of N4BP1 in the pLEX vector could account for differences between the screens in fold-enrichment of N4BP1 and thus interacting proteins. However, differences in buffer concentration could lead to dissociation of real protein interactors from N4BP1, and their exclusion from the data above. It is important to note that it is possible that differences in proteins identified between the U-2 OS and HeLa screens could be explained by variation of localization of N4BP1 or to differences in protein interactions and expression between the cell lines. Thus, while the data from the U-2 OS screen may provide insight into a novel role of N4BP1 in regulating actin dynamics (e.g. via coronin2a and 2b, MISP and PALM) and illustrate that this protein interacts with a yet unidentified E3 ubiquitin ligase, further

experimentation must be done to assess whether these are true N4BP1-interacting partners. Such experiments would include using the same vector and buffer used in the HeLa screen, as well as confirming protein interactions through co-immunoprecipitation assays.

Importantly, the HeLa screen found mitochondrial proteins, as well as proteins native to the secretory and endocytic pathways. Such findings are intriguing, as immunofluorescence data did not show strong localization to these structures (Figures 10-12). It is possible that N4BP1 localizes to these regions but did not accumulate enough to be detected by immunofluorescence. Another possibility is that N4BP1 interacts with these proteins via its role in protein modifications in the nucleus. For example, if the mitochondrial protein CYCS was damaged, it could localize to protein modification sites for turnover or repair. As noted above, while these findings may illustrate new roles of N4BP1, novel protein interactors must be validated using co-immunoprecipitation assays.

Since N4BP1 co-localizes with the P-body protein EDC4, and narrowly missed the significance cut-off for interactions with this protein in both proteomic screens, this project sought to determine whether these proteins physically interact with one another. As such, FLAG-tagged N4BP1 and V5-tagged EDC4 were ectopically expressed in HeLa cells, followed by FLAG immunoprecipitation and western blotting (Figure 15). N4BP1 did not strongly co-immunoprecipitate EDC4, while MARF1, a positive control known to interact directly with EDC4, did (Brothers et a., 2020). While there was slightly more signal in the immunoprecipitation lane compared to the beads-alone control in the N4BP1 expressing samples, it is difficult to determine whether this difference illustrates a weak interaction between N4BP1 and EDC4. These results, along with the fact that N4BP1 co-localize with P-body proteins (Figures 10-12) suggest that N4BP1 is likely to interact with other P-body proteins

directly, or that it may localize to P-bodies via RNA interactions. However, it is possible that N4BP1 does interact directly with EDC4, just not under the conditions used in this experiment.

It was originally hypothesized that N4BP1 localization was dictated by interactions with P-body proteins; however, the data above do not support this hypothesis. While N4BP1 does co-localize with EDC4 and DCP1, and overexpression of EDC4 leads to a decrease in nuclear N4BP1 (Figure 10), proteomic experiments do not show direct binding between N4BP1 and P-body proteins (Figures 13, 14, and 15). It is rather puzzling that N4BP1 can localize to P-bodies without interacting with any proteins found in that region. One likely explanation for this phenomenon is that cells were treated with benzonase, a non-specific ribonuclease, during lysis steps in co-immunoprecipitation and mass spectrometry experiments. This is standard for proteomic experiments, to ensure that proteins identified to interact with N4BP1 are interacting directly, and not via RNA-dependent interactions. It is possible, however, that N4BP1 has cellular roles (e.g. in P-bodies) dependent on these RNA interactions, and thus benzonase treatment disrupts these interactions and excludes RNA dependent roles from the data above. EDC4 was identified in both U-2 OS and HeLa proteomic screens, however, just missing the cut-off for significance. Similarly, LSM12, PABPC4 and PAIP1 are all proteins involved in mRNA regulation that narrowly missed the cutoff in the HeLa screen. Altogether, these findings suggest that N4BP1 may indirectly interact with various mRNA regulating proteins, possibly through RNA dependent interactions. Therefore, assessment of RNA-dependent interactions must be included in future experimentation to assess uncharacterized roles of N4BP1 in RNA regulation.

Conclusions and future directions

There remain some important unanswered questions after this project – does N4BP1 bind to endogenous mRNAs and repress their expression? What dictates N4BP1 localization? What is the role of N4BP1 in P-bodies? To further assess these questions, cross-linking immunoprecipitation and RNA sequencing should be performed using catalytically inactive (ΔNYN) N4BP1 and identified targets should be validated using RT-qPCR. Fragments of N4BP1 assessed in Figures 11 and 12 should be further divided and analyzed using immunofluorescence to elucidate important domains/residues that dictate localization. Furthermore, co-immunoprecipitation studies should be performed to validate identified interacting proteins from mass spectrometry experiments, which could offer important insight into how N4BP1 functions and localizes within cells. Lastly, N4BP1 has a clear role in the immune response (Yamasoba et al., 2019, Gitlin et al., 2020, Shi et al., 2021); further experiments should be conducted to assess how immune stimulation (e.g. using IFN- β) impacts N4BP1 regulation of RNA, localization, and protein interactions.

While the importance of N4BP1 in protein modifications and immune regulation is well documented, the RNA repressing role of N4BP1 has not been thoroughly assessed. This project illustrates that N4BP1 can repress a tethered mRNA dependent on its NYN domain and identified a previously uncharacterized role of N4BP1 in P-bodies. Further, the first large-scale proteomic analysis of N4BP1-protein interactors was carried out, supporting literature findings that N4BP1 regulates protein modification and the immune system (Sharma et al., 2010, Gitlin et al., 2020), while also identifying possible novel roles of N4BP1 in the mitochondria, secretory system, endocytic pathway and in regulating actin dynamics. These findings expand upon the body of knowledge of the relatively uncharacterized protein N4BP1, and offer insight into how

this protein represses targeted mRNAs and exerts its function in the immune system and viral repression.

References

Alles, J., Fehlmann, T., Fischer, U., Backes, C., Galata, V., Minet, M., Hart, M., Abu-Halima, M., Grässer, F. A., Lenhof, H. P., Keller, A., & Meese, E. (2019). An estimate of the total number of true human miRNAs. *Nucleic Acids Res*, *47*(7), 3353-3364. https://doi.org/10.1093/nar/gkz097

Anantharaman, V., & Aravind, L. (2006). The NYN domains: novel predicted RNAses with a PIN domain-like fold. *RNA Biol*, *3*(1), 18-27. https://doi.org/10.4161/rna.3.1.2548

Andrei, M. A., Ingelfinger, D., Heintzmann, R., Achsel, T., Rivera-Pomar, R., & Lührmann, R. (2005). A role for eIF4E and eIF4E-transporter in targeting mRNPs to mammalian processing bodies. *RNA*, *11*(5), 717-727. https://doi.org/10.1261/rna.2340405

Araki, T., & Milbrandt, J. (2003). ZNRF proteins constitute a family of presynaptic E3 ubiquitin ligases. *J Neurosci*, *23*(28), 9385-9394.

Arimoto, K., Fukuda, H., Imajoh-Ohmi, S., Saito, H., & Takekawa, M. (2008). Formation of stress granules inhibits apoptosis by suppressing stress-responsive MAPK pathways. *Nat Cell Biol*, *10*(11), 1324-1332. https://doi.org/10.1038/ncb1791

Beelman, C. A., & Parker, R. (1995). Degradation of mRNA in eukaryotes. *Cell*, *81*(2), 179-183. https://doi.org/10.1016/0092-8674(95)90326-7

Berglund, J. A., Chua, K., Abovich, N., Reed, R., & Rosbash, M. (1997). The splicing factor BBP interacts specifically with the pre-mRNA branchpoint sequence UACUAAC. *Cell*, *89*(5), 781-787. https://doi.org/10.1016/s0092-8674(00)80261-5

Beverly, L. J., Lockwood, W. W., Shah, P. P., Erdjument-Bromage, H., & Varmus, H. (2012). Ubiquitylation, localization, and stability of an anti-apoptotic BCL2-like protein, BCL2L10/BCLb, are regulated by Ubiquilin1. *Proc Natl Acad Sci U S A*, *109*(3), E119-126. https://doi.org/10.1073/pnas.1119167109

Bos, T. J., Nussbacher, J. K., Aigner, S., & Yeo, G. W. (2016). Tethered Function Assays as Tools to Elucidate the Molecular Roles of RNA-Binding Proteins. *Adv Exp Med Biol*, *907*, 61-88. https://doi.org/10.1007/978-3-319-29073-7_3

Bouasker, S., & Simard, M. J. (2012). The slicing activity of miRNA-specific Argonautes is essential for the miRNA pathway in C. elegans. *Nucleic Acids Res*, *40*(20), 10452-10462. https://doi.org/10.1093/nar/gks748

Braddock, D. T., Baber, J. L., Levens, D., & Clore, G. M. (2002). Molecular basis of sequence-specific single-stranded DNA recognition by KH domains: solution structure of a complex between hnRNP K KH3 and single-stranded DNA. *EMBO J*, *21*(13), 3476-3485. https://doi.org/10.1093/emboj/cdf352

Braun, J. E., Tritschler, F., Haas, G., Igreja, C., Truffault, V., Weichenrieder, O., & Izaurralde, E. (2010). The C-terminal alpha-alpha superhelix of Pat is required for mRNA decapping in metazoa. *EMBO J*, *29*(14), 2368-2380. https://doi.org/10.1038/emboj.2010.124

Brengues, M., Teixeira, D., & Parker, R. (2005). Movement of eukaryotic mRNAs between polysomes and cytoplasmic processing bodies. *Science*, *310*(5747), 486-489. https://doi.org/10.1126/science.1115791

Brothers, W. R., Hebert, S., Kleinman, C. L., & Fabian, M. R. (2020). A non-canonical role for the EDC4 decapping factor in regulating MARF1-mediated mRNA decay. *Elife*, *9*. https://doi.org/10.7554/eLife.54995

Burke, J. M., Moon, S. L., Matheny, T., & Parker, R. (2019). RNase L Reprograms Translation by Widespread mRNA Turnover Escaped by Antiviral mRNAs. *Mol Cell*, *75*(6), 1203-1217.e1205. https://doi.org/10.1016/j.molcel.2019.07.029

Bushell, M., & Sarnow, P. (2002). Hijacking the translation apparatus by RNA viruses. *J Cell Biol*, *158*(3), 395-399. https://doi.org/10.1083/jcb.200205044

Cai, J., Yang, L., Wang, B., Huang, Y., Tang, J., Lu, Y., Wu, Z., & Jian, J. (2014). Identification of a novel N4BP1-like gene from grass carp (Ctenopharyngodon idella) in response to GCRV infection. *Fish Shellfish Immunol*, *36*(1), 223-228. https://doi.org/10.1016/j.fsi.2013.11.003

Chambers, D. M., Moretti, L., Zhang, J. J., Cooper, S. W., Santangelo, P. J., & Barker, T. H. (2018). LEM domain-containing protein 3 antagonizes TGFβ-SMAD2/3 signalling in a stiffness-dependent manner in both the nucleus and cytosol. *J Biol Chem*, *293*(41), 15867-15886. https://doi.org/10.1074/jbc.RA118.003658

Chang, C. T., Bercovich, N., Loh, B., Jonas, S., & Izaurralde, E. (2014b). The activation of the decapping enzyme DCP2 by DCP1 occurs on the EDC4 scaffold and involves a conserved loop in DCP1. *Nucleic Acids Res*, *42*(8), 5217-5233. https://doi.org/10.1093/nar/gku129

Cléry, A. A., Frédéric. (2012). FROM STRUCTURE TO FUNCTION OF RNA BINDING DOMAINS. In Z. Lorkovic (Ed.), *RNA Binding Proteins* (1 ed.). Landes Bioscience.

Conte, M. R., Grüne, T., Ghuman, J., Kelly, G., Ladas, A., Matthews, S., & Curry, S. (2000). Structure of tandem RNA recognition motifs from polypyrimidine tract binding protein reveals novel features of the RRM fold. *EMBO J*, *19*(12), 3132-3141. https://doi.org/10.1093/emboj/19.12.3132

Decker, C. J., & Parker, R. (1993). A turnover pathway for both stable and unstable mRNAs in yeast: evidence for a requirement for deadenylation. *Genes Dev*, *7*(8), 1632-1643. https://doi.org/10.1101/gad.7.8.1632

Deo, R. C., Bonanno, J. B., Sonenberg, N., & Burley, S. K. (1999). Recognition of polyadenylate RNA by the poly(A)-binding protein. *Cell*, *98*(6), 835-845. https://doi.org/10.1016/s0092-8674(00)81517-2

Ding, J., Hayashi, M. K., Zhang, Y., Manche, L., Krainer, A. R., & Xu, R. M. (1999). Crystal structure of the two-RRM domain of hnRNP A1 (UP1) complexed with single-stranded telomeric DNA. *Genes Dev*, *13*(9), 1102-1115. https://doi.org/10.1101/gad.13.9.1102

Ding, X. Q., Wang, Z. Y., Xia, D., Wang, R. X., Pan, X. R., & Tong, J. H. (2020). Proteomic Profiling of Serum Exosomes From Patients With Metastatic Gastric Cancer. *Front Oncol*, *10*, 1113. https://doi.org/10.3389/fonc.2020.01113

Du, Z., Lee, J. K., Fenn, S., Tjhen, R., Stroud, R. M., & James, T. L. (2007). X-ray crystallographic and NMR studies of protein-protein and protein-nucleic acid interactions involving the KH domains from human poly(C)-binding protein-2. *RNA*, *13*(7), 1043-1051. https://doi.org/10.1261/rna.410107

Eberle, A. B., Lykke-Andersen, S., Mühlemann, O., & Jensen, T. H. (2009). SMG6 promotes endonucleolytic cleavage of nonsense mRNA in human cells. *Nat Struct Mol Biol*, *16*(1), 49-55. https://doi.org/10.1038/nsmb.1530

Ender, C., & Meister, G. (2010). Argonaute proteins at a glance. *J Cell Sci*, *123*(Pt 11), 1819-1823. https://doi.org/10.1242/jcs.055210

Eulalio, A., Behm-Ansmant, I., Schweizer, D., & Izaurralde, E. (2007). P-body formation is a consequence, not the cause, of RNA-mediated gene silencing. *Mol Cell Biol*, *27*(11), 3970-3981. https://doi.org/10.1128/MCB.00128-07

Ficarelli, M., Wilson, H., Pedro Galão, R., Mazzon, M., Antzin-Anduetza, I., Marsh, M., Neil, S. J., & Swanson, C. M. (2019). KHNYN is essential for the zinc finger antiviral protein (ZAP) to restrict HIV-1 containing clustered CpG dinucleotides. *Elife*, *8*. https://doi.org/10.7554/eLife.46767

Figliuolo da Paz, V., Ghishan, F. K., & Kiela, P. R. (2020). Emerging Roles of Disabled Homolog 2 (DAB2) in Immune Regulation. *Front Immunol*, *11*, 580302. https://doi.org/10.3389/fimmu.2020.580302

Fischer, E. S., Böhm, K., Lydeard, J. R., Yang, H., Stadler, M. B., Cavadini, S., Nagel, J., Serluca, F., Acker, V., Lingaraju, G. M., Tichkule, R. B., Schebesta, M., Forrester, W. C., Schirle, M., Hassiepen, U., Ottl, J., Hild, M., Beckwith, R. E., Harper, J. W., Jenkins, J. L., & Thomä, N. H. (2014). Structure of the DDB1-CRBN E3 ubiquitin ligase in complex with thalidomide. *Nature*, *512*(7512), 49-53. https://doi.org/10.1038/nature13527

Garg, A., Roske, Y., Yamada, S., Uehata, T., Takeuchi, O., & Heinemann, U. (2021). PIN and CCCH Zn-finger domains coordinate RNA targeting in ZC3H12 family endoribonucleases. *Nucleic Acids Res*, *49*(9), 5369-5381. https://doi.org/10.1093/nar/gkab316

Gitlin, A. D., Heger, K., Schubert, A. F., Reja, R., Yan, D., Pham, V. C., Suto, E., Zhang, J., Kwon, Y. C., Freund, E. C., Kang, J., Pham, A., Caothien, R., Bacarro, N., Hinkle, T., Xu, M., McKenzie, B. S., Haley, B., Lee, W. P., Lill, J. R., Roose-Girma, M., Dohse, M., Webster, J. D., Newton, K., & Dixit, V. M. (2020). Integration of innate immune signalling by caspase-8 cleavage of N4BP1. *Nature*, *587*(7833), 275-280. https://doi.org/10.1038/s41586-020-2796-5

Glavan, F., Behm-Ansmant, I., Izaurralde, E., & Conti, E. (2006). Structures of the PIN domains of SMG6 and SMG5 reveal a nuclease within the mRNA surveillance complex. *EMBO J*, *25*(21), 5117-5125. https://doi.org/10.1038/sj.emboj.7601377

Gollob, J. A., Li, J., Kawasaki, H., Daley, J. F., Groves, C., Reinherz, E. L., & Ritz, J. (1996). Molecular interaction between CD58 and CD2 counter-receptors mediates the ability of monocytes to augment T cell activation by IL-12. *J Immunol*, *157*(5), 1886-1893.

Goodier, J. L., Pereira, G. C., Cheung, L. E., Rose, R. J., & Kazazian, H. H. (2015). The Broad-Spectrum Antiviral Protein ZAP Restricts Human Retrotransposition. *PLoS Genet*, *11*(5), e1005252. https://doi.org/10.1371/journal.pgen.1005252

Harigaya, Y., & Parker, R. (2010). No-go decay: a quality control mechanism for RNA in translation. *Wiley Interdiscip Rev RNA*, *1*(1), 132-141. https://doi.org/10.1002/wrna.17

Howard, M. J., Klemm, B. P., & Fierke, C. A. (2015). Mechanistic Studies Reveal Similar Catalytic Strategies for Phosphodiester Bond Hydrolysis by Protein-only and RNA-dependent Ribonuclease P. *J Biol Chem*, *290*(21), 13454-13464. https://doi.org/10.1074/jbc.M115.644831

Hubel, P., Urban, C., Bergant, V., Schneider, W. M., Knauer, B., Stukalov, A., Scaturro, P., Mann, A., Brunotte, L., Hoffmann, H. H., Schoggins, J. W., Schwemmle, M., Mann, M., Rice, C. M., & Pichlmair, A. (2019). A protein-interaction network of interferon-stimulated genes extends the innate immune system landscape. *Nat Immunol*, *20*(4), 493-502. https://doi.org/10.1038/s41590-019-0323-3

Ivashkiv, L. B., & Donlin, L. T. (2014). Regulation of type I interferon responses. *Nat Rev Immunol*, *14*(1), 36-49. https://doi.org/10.1038/nri3581

Jang, D., Kwon, H., Choi, M., Lee, J., & Pak, Y. (2019). Sumoylation of Flotillin-1 promotes EMT in metastatic prostate cancer by suppressing Snail degradation. *Oncogene*, *38*(17), 3248-3260. https://doi.org/10.1038/s41388-018-0641-1

Jeltsch, K. M., Hu, D., Brenner, S., Zöller, J., Heinz, G. A., Nagel, D., Vogel, K. U., Rehage, N., Warth, S. C., Edelmann, S. L., Gloury, R., Martin, N., Lohs, C., Lech, M., Stehklein, J. E., Geerlof, A., Kremmer, E., Weber, A., Anders, H. J., Schmitz, I., Schmidt-Supprian, M., Fu, M., Holtmann, H., Krappmann, D., Ruland, J., Kallies, A., Heikenwalder, M., & Heissmeyer, V. (2014). Cleavage of roquin and regnase-1 by the paracaspase MALT1 releases their cooperatively repressed targets to promote T(H)17 differentiation. *Nat Immunol*, *15*(11), 1079-1089. https://doi.org/10.1038/ni.3008

Karousis, E. D., Nasif, S., & Mühlemann, O. (2016). Nonsense-mediated mRNA decay: novel mechanistic insights and biological impact. *Wiley Interdiscip Rev RNA*, *7*(5), 661-682. https://doi.org/10.1002/wrna.1357

Kedersha, N., Cho, M. R., Li, W., Yacono, P. W., Chen, S., Gilks, N., Golan, D. E., & Anderson, P. (2000). Dynamic shuttling of TIA-1 accompanies the recruitment of mRNA to mammalian stress granules. *J Cell Biol*, *151*(6), 1257-1268. https://doi.org/10.1083/jcb.151.6.1257

Kedersha, N., Gupta, M., Li, W., Miller, I., & Anderson, P. (1999). RNA-binding proteins TIA-1 and TIAR link the phosphorylation of eIF-2 alpha to the assembly of mammalian stress granules. *J Cell Biol*, *147*(7), 1431-1442. https://doi.org/10.1083/jcb.147.7.1431

Kedersha, N., Stoecklin, G., Ayodele, M., Yacono, P., Lykke-Andersen, J., Fritzler, M. J., Scheuner, D., Kaufman, R. J., Golan, D. E., & Anderson, P. (2005). Stress granules and processing bodies are dynamically linked sites of mRNP remodeling. *J Cell Biol*, *169*(6), 871-884. https://doi.org/10.1083/jcb.200502088

Khong, A., Matheny, T., Jain, S., Mitchell, S. F., Wheeler, J. R., & Parker, R. (2017). The Stress Granule Transcriptome Reveals Principles of mRNA Accumulation in Stress Granules. *Mol Cell*, *68*(4), 808-820.e805. https://doi.org/10.1016/j.molcel.2017.10.015

Kini, H. K., Kong, J., & Liebhaber, S. A. (2014). Cytoplasmic poly(A) binding protein C4 serves a critical role in erythroid differentiation. *Mol Cell Biol*, *34*(7), 1300-1309. https://doi.org/10.1128/MCB.01683-13

Kulkarni, M., Ozgur, S., & Stoecklin, G. (2010). On track with P-bodies. *Biochem Soc Trans*, *38*(Pt 1), 242-251. https://doi.org/10.1042/BST0380242

Lallemand-Breitenbach, V., Jeanne, M., Benhenda, S., Nasr, R., Lei, M., Peres, L., Zhou, J., Zhu, J., Raught, B., & de Thé, H. (2008). Arsenic degrades PML or PML-RARalpha through a SUMO-triggered RNF4/ubiquitin-mediated pathway. *Nat Cell Biol*, *10*(5), 547-555. https://doi.org/10.1038/ncb1717

Leroy, M., Piton, J., Gilet, L., Pellegrini, O., Proux, C., Coppée, J. Y., Figaro, S., & Condon, C. (2017). Rae1/YacP, a new endoribonuclease involved in ribosome-dependent mRNA decay in. *EMBO J*, *36*(9), 1167-1181. https://doi.org/10.15252/embj.201796540

Liu, J., Carmell, M. A., Rivas, F. V., Marsden, C. G., Thomson, J. M., Song, J. J., Hammond, S. M., Joshua-Tor, L., & Hannon, G. J. (2004). Argonaute2 is the catalytic engine of mammalian RNAi. *Science*, *305*(5689), 1437-1441. https://doi.org/10.1126/science.1102513

Liu, S., Qiu, C., Miao, R., Zhou, J., Lee, A., Liu, B., Lester, S. N., Fu, W., Zhu, L., Zhang, L., Xu, J., Fan, D., Li, K., Fu, M., & Wang, T. (2013). MCPIP1 restricts HIV infection and is rapidly degraded in activated CD4+ T cells. *Proc Natl Acad Sci U S A*, *110*(47), 19083-19088. https://doi.org/10.1073/pnas.1316208110

Liu, Y. Z., Yang, H., Cao, J., Jiang, Y. Y., Hao, J. J., Xu, X., Cai, Y., & Wang, M. R. (2016). KIAA1522 is a novel prognostic biomarker in patients with non-small cell lung cancer. *Sci Rep*, *6*, 24786. https://doi.org/10.1038/srep24786

Losson, R., & Lacroute, F. (1979). Interference of nonsense mutations with eukaryotic messenger RNA stability. *Proc Natl Acad Sci U S A*, *76*(10), 5134-5137. https://doi.org/10.1073/pnas.76.10.5134

Luo, Y., Na, Z., & Slavoff, S. A. (2018b). P-Bodies: Composition, Properties, and Functions. *Biochemistry*, *57*(17), 2424-2431. https://doi.org/10.1021/acs.biochem.7b01162

Lv, Y., Zhang, K., & Gao, H. (2014). Paip1, an effective stimulator of translation initiation, is targeted by WWP2 for ubiquitylation and degradation. *Mol Cell Biol*, *34*(24), 4513-4522. https://doi.org/10.1128/MCB.00524-14

Mao, G., Chen, T. H., Srivastava, A. S., Kosek, D., Biswas, P. K., Gopalan, V., & Kirsebom, L. A. (2016). Cleavage of Model Substrates by Arabidopsis thaliana PRORP1 Reveals New Insights into Its Substrate Requirements. *PLoS One*, *11*(8), e0160246. https://doi.org/10.1371/journal.pone.0160246

Matsushita, K., Takeuchi, O., Standley, D. M., Kumagai, Y., Kawagoe, T., Miyake, T., Satoh, T., Kato, H., Tsujimura, T., Nakamura, H., & Akira, S. (2009). Zc3h12a is an RNase essential for controlling immune responses by regulating mRNA decay. *Nature*, *458*(7242), 1185-1190. https://doi.org/10.1038/nature07924

Mellacheruvu, D., Wright, Z., Couzens, A. L., Lambert, J. P., St-Denis, N. A., Li, T., Miteva, Y. V., Hauri, S., Sardiu, M. E., Low, T. Y., Halim, V. A., Bagshaw, R. D., Hubner, N. C., Al-Hakim, A., Bouchard, A., Faubert, D., Fermin, D., Dunham, W. H., Goudreault, M., Lin, Z. Y., Badillo, B. G., Pawson, T., Durocher, D., Coulombe, B., Aebersold, R., Superti-Furga, G., Colinge, J., Heck, A. J., Choi, H., Gstaiger, M., Mohammed, S., Cristea, I. M., Bennett, K. L., Washburn, M. P., Raught, B., Ewing, R. M., Gingras, A. C., & Nesvizhskii, A. I. (2013). The CRAPome: a contaminant repository for affinity purification-mass spectrometry data. *Nat Methods*, *10*(8), 730-736. https://doi.org/10.1038/nmeth.2557

Mino, T., & Takeuchi, O. (2015). Regnase-1 and Roquin regulate inflammatory mRNAs. *Oncotarget*, *6*(20), 17869-17870. https://doi.org/10.18632/oncotarget.4891

Mollet, S., Cougot, N., Wilczynska, A., Dautry, F., Kress, M., Bertrand, E., & Weil, D. (2008). Translationally repressed mRNA transiently cycles through stress granules during stress. *Mol Biol Cell*, *19*(10), 4469-4479. https://doi.org/10.1091/mbc.e08-05-0499

Moreno-Oñate, M., Herrero-Ruiz, A. M., García-Dominguez, M., Cortés-Ledesma, F., & Ruiz, J. F. (2020). RanBP2-Mediated SUMOylation Promotes Human DNA Polymerase Lambda Nuclear Localization and DNA Repair. *J Mol Biol*, *432*(13), 3965-3979. https://doi.org/10.1016/j.jmb.2020.03.020

Morozova, N., Allers, J., Myers, J., & Shamoo, Y. (2006). Protein-RNA interactions: exploring binding patterns with a three-dimensional superposition analysis of high resolution structures. *Bioinformatics*, *22*(22), 2746-2752. https://doi.org/10.1093/bioinformatics/btl470

Muhlrad, D., Decker, C. J., & Parker, R. (1994). Deadenylation of the unstable mRNA encoded by the yeast MFA2 gene leads to decapping followed by 5'-->3' digestion of the transcript. *Genes Dev*, *8*(7), 855-866. https://doi.org/10.1101/gad.8.7.855

Nagai, T., Mukoyama, S., Kagiwada, H., Goshima, N., & Mizuno, K. (2018). Cullin-3-KCTD10-mediated CEP97 degradation promotes primary cilium formation. *J Cell Sci*, *131*(24). https://doi.org/10.1242/jcs.219527

Nepravishta, R., Ferrentino, F., Mandaliti, W., Mattioni, A., Weber, J., Polo, S., Castagnoli, L., Cesareni, G., Paci, M., & Santonico, E. (2019). Erratum: Nepravishta, R., et al. CoCUN, a Novel Ubiquitin Binding Domain Identified in N4BP1. *Biomolecules*, *9*(12). https://doi.org/10.3390/biom9120803

Nishimura, T., Fakim, H., Brandmann, T., Youn, J. Y., Gingras, A. C., Jinek, M., & Fabian, M. R. (2018). Human MARF1 is an endoribonuclease that interacts with the DCP1:2 decapping complex and degrades target mRNAs. *Nucleic Acids Res*, *46*(22), 12008-12021. https://doi.org/10.1093/nar/gky1011

Novoa, I., Zeng, H., Harding, H. P., & Ron, D. (2001). Feedback inhibition of the unfolded protein response by GADD34-mediated dephosphorylation of eIF2alpha. *J Cell Biol*, *153*(5), 1011-1022. https://doi.org/10.1083/jcb.153.5.1011

Oberst, A., Malatesta, M., Aqeilan, R. I., Rossi, M., Salomoni, P., Murillas, R., Sharma, P., Kuehn, M. R., Oren, M., Croce, C. M., Bernassola, F., & Melino, G. (2007). The Nedd4-binding partner 1 (N4BP1) protein is an inhibitor of the E3 ligase Itch. *Proc Natl Acad Sci U S A*, *104*(27), 11280-11285. https://doi.org/10.1073/pnas.0701773104

Osakabe, A., Tachiwana, H., Takaku, M., Hori, T., Obuse, C., Kimura, H., Fukagawa, T., & Kurumizaka, H. (2013). Vertebrate Spt2 is a novel nucleolar histone chaperone that

assists in ribosomal DNA transcription. *J Cell Sci*, *126*(Pt 6), 1323-1332. https://doi.org/10.1242/jcs.112623

Ow, Y. P., Green, D. R., Hao, Z., & Mak, T. W. (2008). Cytochrome c: functions beyond respiration. *Nat Rev Mol Cell Biol*, *9*(7), 532-542. https://doi.org/10.1038/nrm2434

Ozgur, S., Chekulaeva, M., & Stoecklin, G. (2010). Human Pat1b connects deadenylation with mRNA decapping and controls the assembly of processing bodies. *Mol Cell Biol*, *30*(17), 4308-4323. https://doi.org/10.1128/MCB.00429-10

Plambeck, C. A., Kwan, A. H., Adams, D. J., Westman, B. J., van der Weyden, L., Medcalf, R. L., Morris, B. J., & Mackay, J. P. (2003). The structure of the zinc finger domain from human splicing factor ZNF265 fold. *J Biol Chem*, *278*(25), 22805-22811. https://doi.org/10.1074/jbc.M301896200

Rocha-Perugini, V., Gordon-Alonso, M., & Sánchez-Madrid, F. (2017). Role of Drebrin at the Immunological Synapse. *Adv Exp Med Biol*, *1006*, 271-280. https://doi.org/10.1007/978-4-431-56550-5_15

Santonico, E. (2020). Old and New Concepts in Ubiquitin and NEDD8 Recognition. *Biomolecules*, *10*(4). https://doi.org/10.3390/biom10040566

Scheuner, D., Song, B., McEwen, E., Liu, C., Laybutt, R., Gillespie, P., Saunders, T., Bonner-Weir, S., & Kaufman, R. J. (2001). Translational control is required for the unfolded protein response and in vivo glucose homeostasis. *Mol Cell*, *7*(6), 1165-1176. https://doi.org/10.1016/s1097-2765(01)00265-9

Schittek, B. (2012). The multiple facets of dermcidin in cell survival and host defense. *J Innate Immun*, *4*(4), 349-360. https://doi.org/10.1159/000336844

Schwarz, A., Möller-Hackbarth, K., Ebarasi, L., Unnersjö Jess, D., Zambrano, S., Blom, H., Wernerson, A., Lal, M., & Patrakka, J. (2019). Coro2b, a podocyte protein downregulated in human diabetic nephropathy, is involved in the development of protamine sulphate-induced foot process effacement. *Sci Rep*, *9*(1), 8888. https://doi.org/10.1038/s41598-019-45303-y

Schäfer, I. B., Yamashita, M., Schuller, J. M., Schüssler, S., Reichelt, P., Strauss, M., & Conti, E. (2019). Molecular Basis for poly(A) RNP Architecture and Recognition by the Pan2-Pan3 Deadenylase. *Cell*, *177*(6), 1619-1631.e1621. https://doi.org/10.1016/j.cell.2019.04.013

Sharma, P., Murillas, R., Zhang, H., & Kuehn, M. R. (2010). N4BP1 is a newly identified nucleolar protein that undergoes SUMO-regulated polyubiquitylation and proteasomal turnover at promyelocytic leukemia nuclear bodies. *J Cell Sci*, *123*(Pt 8), 1227-1234. https://doi.org/10.1242/jcs.060160

Shaw, A. E., Hughes, J., Gu, Q., Behdenna, A., Singer, J. B., Dennis, T., Orton, R. J., Varela, M., Gifford, R. J., Wilson, S. J., & Palmarini, M. (2017). Fundamental properties of the mammalian innate immune system revealed by multispecies comparison of type I interferon responses. *PLoS Biol*, *15*(12), e2004086. https://doi.org/10.1371/journal.pbio.2004086

Shi, H., Sun, L., Wang, Y., Liu, A., Zhan, X., Li, X., Tang, M., Anderton, P., Hildebrand, S., Quan, J., Ludwig, S., Moresco, E. M. Y., & Beutler, B. (2021). N4BP1 negatively regulates NF-κB by binding and inhibiting NEMO oligomerization. *Nat Commun*, *12*(1), 1379. https://doi.org/10.1038/s41467-021-21711-5

Shi, X., & Wang, X. (2015). The role of MTDH/AEG-1 in the progression of cancer. *Int J Clin Exp Med*, *8*(4), 4795-4807.

Solinger, J. A., Pascolini, D., & Heyer, W. D. (1999). Active-site mutations in the Xrn1p exoribonuclease of Saccharomyces cerevisiae reveal a specific role in meiosis. *Mol Cell Biol*, *19*(9), 5930-5942. https://doi.org/10.1128/MCB.19.9.5930

Spel, L., Nieuwenhuis, J., Haarsma, R., Stickel, E., Bleijerveld, O. B., Altelaar, M., Boelens, J. J., Brummelkamp, T. R., Nierkens, S., & Boes, M. (2018). Nedd4-Binding Protein 1 and TNFAIP3-Interacting Protein 1 Control MHC-1 Display in Neuroblastoma. *Cancer Res*, *78*(23), 6621-6631. https://doi.org/10.1158/0008-5472.CAN-18-0545

Stadler, M., Chelbi-Alix, M. K., Koken, M. H., Venturini, L., Lee, C., Saïb, A., Quignon, F., Pelicano, L., Guillemin, M. C., & Schindler, C. (1995). Transcriptional induction of the PML growth suppressor gene by interferons is mediated through an ISRE and a GAS element. *Oncogene*, *11*(12), 2565-2573.

Su, Y. Q., Sugiura, K., Sun, F., Pendola, J. K., Cox, G. A., Handel, M. A., Schimenti, J. C., & Eppig, J. J. (2012). MARF1 regulates essential oogenic processes in mice. *Science*, *335*(6075), 1496-1499. https://doi.org/10.1126/science.1214680

Sun, H., Lagarrigue, F., Wang, H., Fan, Z., Lopez-Ramirez, M. A., Chang, J. T., & Ginsberg, M. H. (2021). Distinct integrin activation pathways for effector and regulatory T cell trafficking and function. *J Exp Med*, *218*(2). https://doi.org/10.1084/jem.20201524

Swisher, K. D., & Parker, R. (2010). Localization to, and effects of Pbp1, Pbp4, Lsm12, Dhh1, and Pab1 on stress granules in Saccharomyces cerevisiae. *PLoS One*, *5*(4), e10006. https://doi.org/10.1371/journal.pone.0010006

Takeuchi, O. (2018). Endonuclease Regnase-1/Monocyte chemotactic protein-1-induced protein-1 (MCPIP1) in controlling immune responses and beyond. *Wiley Interdiscip Rev RNA*, *9*(1). https://doi.org/10.1002/wrna.1449

Teplova, M., & Patel, D. J. (2008). Structural insights into RNA recognition by the alternative-splicing regulator muscleblind-like MBNL1. *Nat Struct Mol Biol*, *15*(12), 1343-1351. https://doi.org/10.1038/nsmb.1519

Tharun, S. (2009). Lsm1-7-Pat1 complex: a link between 3' and 5'-ends in mRNA decay? *RNA Biol*, *6*(3), 228-232. https://doi.org/10.4161/rna.6.3.8282

Tourrière, H., Chebli, K., Zekri, L., Courselaud, B., Blanchard, J. M., Bertrand, E., & Tazi, J. (2003). The RasGAP-associated endoribonuclease G3BP assembles stress granules. *J Cell Biol*, *160*(6), 823-831. https://doi.org/10.1083/jcb.200212128

Turk, C. M., Fagan-Solis, K. D., Williams, K. E., Gozgit, J. M., Smith-Schneider, S., Marconi, S. A., Otis, C. N., Crisi, G. M., Anderton, D. L., Kilimann, M. W., & Arcaro, K. F. (2012). Paralemmin-1 is over-expressed in estrogen-receptor positive breast cancers. *Cancer Cell Int*, *12*(1), 17. https://doi.org/10.1186/1475-2867-12-17

Uehata, T., Iwasaki, H., Vandenbon, A., Matsushita, K., Hernandez-Cuellar, E., Kuniyoshi, K., Satoh, T., Mino, T., Suzuki, Y., Standley, D. M., Tsujimura, T., Rakugi, H., Isaka, Y., Takeuchi, O., & Akira, S. (2013). Malt1-induced cleavage of regnase-1 in CD4(+) helper T cells regulates immune activation. *Cell*, *153*(5), 1036-1049. https://doi.org/10.1016/j.cell.2013.04.034

Uehata, T., & Takeuchi, O. (2020). RNA Recognition and Immunity-Innate Immune Sensing and Its Posttranscriptional Regulation Mechanisms. *Cells*, *9*(7). https://doi.org/10.3390/cells9071701

Valverde, R., Edwards, L., & Regan, L. (2008). Structure and function of KH domains. *FEBS J*, *275*(11), 2712-2726. https://doi.org/10.1111/j.1742-4658.2008.06411.x

Wang, C., Schmich, F., Srivatsa, S., Weidner, J., Beerenwinkel, N., & Spang, A. (2018). Correction: Context-dependent deposition and regulation of mRNAs in P-bodies. *Elife*, *7*. https://doi.org/10.7554/eLife.41300

Wang, Z., Zhang, H., & Cheng, Q. (2020). PDIA4: The basic characteristics, functions and its potential connection with cancer. *Biomed Pharmacother*, *122*, 109688. https://doi.org/10.1016/j.biopha.2019.109688

Yamasoba, D., Sato, K., Ichinose, T., Imamura, T., Koepke, L., Joas, S., Reith, E., Hotter, D., Misawa, N., Akaki, K., Uehata, T., Mino, T., Miyamoto, S., Noda, T., Yamashita, A., Standley, D. M., Kirchhoff, F., Sauter, D., Koyanagi, Y., & Takeuchi, O. (2019). N4BP1 restricts HIV-1 and its inactivation by MALT1 promotes viral reactivation. *Nat Microbiol*, *4*(9), 1532-1544. https://doi.org/10.1038/s41564-019-0460-3

Yi, H., Park, J., Ha, M., Lim, J., Chang, H., & Kim, V. N. (2018). PABP Cooperates with the CCR4-NOT Complex to Promote mRNA Deadenylation and Block Precocious Decay. *Mol Cell*, *70*(6), 1081-1088.e1085. https://doi.org/10.1016/j.molcel.2018.05.009

Yokogawa, M., Tsushima, T., Noda, N. N., Kumeta, H., Enokizono, Y., Yamashita, K., Standley, D. M., Takeuchi, O., Akira, S., & Inagaki, F. (2016). Structural basis for the regulation of enzymatic activity of Regnase-1 by domain-domain interactions. *Sci Rep*, *6*, 22324. https://doi.org/10.1038/srep22324

Youn, J. Y., Dunham, W. H., Hong, S. J., Knight, J. D. R., Bashkurov, M., Chen, G. I., Bagci, H., Rathod, B., MacLeod, G., Eng, S. W. M., Angers, S., Morris, Q., Fabian, M., Côté, J. F., & Gingras, A. C. (2018). High-Density Proximity Mapping Reveals the Subcellular Organization of mRNA-Associated Granules and Bodies. *Mol Cell*, *69*(3), 517-532.e511. https://doi.org/10.1016/j.molcel.2017.12.020

Zhu, M., Settele, F., Kotak, S., Sanchez-Pulido, L., Ehret, L., Ponting, C. P., Gönczy, P., & Hoffmann, I. (2013). MISP is a novel Plk1 substrate required for proper spindle orientation and mitotic progression. *J Cell Biol*, *200*(6), 773-787. https://doi.org/10.1083/jcb.201207050

Zipprich, J. T., Bhattacharyya, S., Mathys, H., & Filipowicz, W. (2009). Importance of the C-terminal domain of the human GW182 protein TNRC6C for translational repression. *RNA*, *15*(5), 781-793. https://doi.org/10.1261/rna.1448009

Łabno, A., Tomecki, R., & Dziembowski, A. (2016). Cytoplasmic RNA decay pathways - Enzymes and mechanisms. *Biochim Biophys Acta*, *1863*(12), 3125-3147. https://doi.org/10.1016/j.bbamcr.2016.09.023

Appendix A

Table 1: **Raw data produced from immunoprecipitation-mass spectrometry of stably expressed V5-N4BP1 in U-2 OS cells.** The data from this table was used to generate Figure 13.

Gene Symbol	Description	Sample/ control	p-value
N4BP1	NEDD4-binding protein 1	56.98	8.95E-03
KIAA1522	Uncharacterized protein KIAA1522	13.83	2.96E-04
EFR3A	Protein EFR3 homolog A	6.71	1.33E-02
CORO2A	Coronin-2A	6.49	2.32E-03
PPP1R18	Phostensin	5.81	2.57E-02
CORO2B	Coronin-2B	5.26	2.94E-03
GLIPR2	Golgi-associated plant pathogenesis-related protein 1	5.25	9.44E-03
C19orf21; MISP	Mitotic interactor and substrate of PLK1	4.02	2.32E-02
PALM	Paralemmin-1	3.93	1.01E-02
GPRC5A	Retinoic acid-induced protein 3	3.81	1.17E-02
FLOT1	Flotillin-1	3.74	2.12E-02
RAPH1	ociated and pleckstrin homology domains-containing p	3.48	1.55E-02
CD58	Lymphocyte function-associated antigen 3	3.37	2.44E-02
PI4KA	Phosphatidylinositol 4-kinase alpha	3.33	6.26E-04
FAM120C	Constitutive coactivator of PPAR-gamma-like protein 2	2.96	7.37E-04
RAC1	Ras-related C3 botulinum toxin substrate 1	2.86	1.44E-02
CD55	Complement decay-accelerating factor	2.49	3.35E-02
CD59	CD59 glycoprotein	2.47	3.40E-02
PIP4K2A	Phosphatidylinositol 5-phosphate 4-kinase type-2 alpha	2.17	1.15E-02
RFWD3	E3 ubiquitin-protein ligase RFWD3	2.10	4.30E-02
STOM	Erythrocyte band 7 integral membrane protein	2.06	3.56E-02
SHCBP1	SHC SH2 domain-binding protein 1	2.06	4.56E-03

Table 2: **Raw data produced from immunoprecipitation-mass spectrometry of stably expressed V5-N4BP1 in HeLa cells.** The data from this table was used to generate Figure 14.

Gene Symbol	Description	CRAPOME Av. SC	# Protein Unique Peptides	Sample/ control	p-value	Candidate	Coverage [%]
LEMD3	Inner nuclear membrane protein Man1	3.4	2	100.00	1.61E-16	high	5
SPTY2D1	Protein SPT2 homolog	1.3	2	100.00	1.61E-16	high	10
DAB2	Disabled homolog 2	7.1	2	100.00	1.61E-16	medium	3
MTDH	Protein LYRIC	5.7	2	100.00	1.61E-16	medium	4
PYM1	Partner of Y14 and mago	2.4	3	100.00	1.61E-16	high	32
CYCS	Cytochrome c	3.3	2	100.00	1.61E-16	high	11
CDKN2AIP	CDKN2A-interacting protein	3.1	2	100.00	1.61E-16	high	7
N4BP1	Nedd4-binding protein 1	2.4	68	100.00	1.61E-16		63
CLINT1	Clathrin interactor 1	8.5	2	100.00	1.61E-16	medium	5
KCTD10	BTB/POZ domain-containing adapter for CUL3-mediated RhoA degradation protein 3	4	2	25.45	2.63E-05	high	8
CYBRD1	Cytochrome b reductase 1	1.5	2	20.83	1.21E-04	high	4
PRKCSH	Glucosidase 2 subunit beta	5.2	3	20.76	1.23E-04	medium	7
DDB1	DNA damage-binding protein 1	6.9	4	20.36	1.41E-04	medium	5
BMP2K	BMP-2-inducible protein kinase	1.7	5	19.48	1.92E-04	high	8
PDIA4	Protein disulfide-isomerase A4	8.8	4	19.41	1.95E-04	medium	9
LARP4	La-related protein 4	1.8	4	18.58	2.66E-04	high	12
EML4	Echinoderm microtubule-associated protein-like 4	1.8	2	14.50	1.35E-03	high	4
SRGAP2	SLIT-ROBO Rho GTPase-activating protein 2	1.8	2	12.50	3.40E-03	high	3
OGFR	Opioid growth factor receptor	1.9	4	12.36	3.55E-03	high	11
GNAI3	Guanine nucleotide-binding protein G(i) subunit alpha	2.8	2	11.31	5.67E-03	high	17
RPL11	60S ribosomal protein L11	4.7	2	11.12	6.23E-03	high	14
CACNA2D1	Voltage-dependent calcium channel subunit alpha-2/delta-1	3.6	3	10.76	7.46E-03	high	5
PPP1R13L	RelA-associated inhibitor	3.3	2	10.72	7.57E-03	high	3
DBNL	Drebrin-like protein	4.4	4	10.33	9.27E-03	high	13

Gene Symbol	Description	CRAPOME Av. SC	# Protein Unique Peptides	Sample/ control	p-value	Candidate	Coverage [%]
DCD	Dermcidin	3.7	2	9.60	1.34E-02	high	24
DYNC1LI2	Cytoplasmic dynein 1 light intermediate chain 2	2.2	4	9.36	1.53E-02	high	7
VAPA	Vesicle-associated membrane protein-associated protein A	2.2	3	9.06	1.81E-02	high	22
SAFB	Scaffold attachment factor B1	6.6	5	8.02	3.29E-02	medium	8
FKBP4	Peptidyl-prolyl cis-trans isomerase FKBP4	8.2	2	7.66	4.04E-02	medium	9
GTF2F1	General transcription factor IIF subunit 1	3.8	2	7.48	4.40E-02	high	8